Journal of Medicinal Chemistry
Article

J. Med. Chem. **2010,** *53,* 5213–5228 **5213**
DOI: 10.1021/jm100262j

Imidazo[4,5-*b*]pyridine Derivatives As Inhibitors of Aurora Kinases: Lead Optimization Studies toward the Identification of an Orally Bioavailable Preclinical Development Candidate‡

Vassilios Bavetsias,*,† Jonathan M. Large,† Chongbo Sun,† Nathalie Bouloc,† Magda Kosmopoulou,# Mizio Matteucci,† Nicola E. Wilsher,† Vanessa Martins,† Jóhannes Reynisson,† Butrus Atrash,† Amir Faisal,† Frederique Urban,† Melanie Valenti,† Alexis de Haven Brandon,† Gary Box,† Florence I. Raynaud,† Paul Workman,† Suzanne A. Eccles,† Richard Bayliss,# Julian Blagg,† Spiros Linardopoulos,†,§ and Edward McDonald*,†

†*Cancer Research UK Centre for Cancer Therapeutics, The Institute of Cancer Research, 15 Cotswold Road, Sutton, Surrey, SM2 5NG, United Kingdom,* #*Section of Structural Biology, The Institute of Cancer Research, Chester Beatty Laboratories, 237 Fulham Road, London, SW3 6JB, United Kingdom, and* §*The Breakthrough Breast Cancer Research Centre, The Institute of Cancer Research, Fulham Road, London SW3 6JB, United Kingdom*

Received February 26, 2010

Lead optimization studies using **7** as the starting point led to a new class of imidazo[4,5-*b*]pyridine-based inhibitors of Aurora kinases that possessed the 1-benzylpiperazinyl motif at the 7-position, and displayed favorable in vitro properties. Cocrystallization of Aurora-A with **40c** (CCT137444) provided a clear understanding into the interactions of this novel class of inhibitors with the Aurora kinases. Subsequent physicochemical property refinement by the incorporation of solubilizing groups led to the identification of 3-((4-(6-bromo-2-(4-(4-methylpiperazin-1-yl)phenyl)-3*H*-imidazo[4,5-*b*]pyridin-7-yl)-piperazin-1-yl)methyl)-5-methylisoxazole (**51**, CCT137690) which is a potent inhibitor of Aurora kinases (Aurora-A IC_{50} = 0.015 ± 0.003 μM, Aurora-B IC_{50} = 0.025 μM, Aurora-C IC_{50} = 0.019 μM). Compound **51** is highly orally bioavailable, and in in vivo efficacy studies it inhibited the growth of SW620 colon carcinoma xenografts following oral administration with no observed toxicities as defined by body weight loss.

Introduction

Aurora proteins A, B, and C, a small family of serine/threonine kinases, play distinct roles in the regulation of mitosis.[1−3] Aurora-A is localized to the spindle poles and spindle microtubules proximal to the centrosomes and is required for centrosome maturation, whereas Aurora-B is localized to kinetochores and is essential for chromosome segregation and cytokinesis.[3] Aurora-B interacts with a number of chromosomal passenger proteins including the inner centromere protein (INCENP[a])[4] and is known to phosphorylate histone H3 during mitosis.[5] These findings generated a considerable interest in the involvement of Aurora kinases in cancer causation and progression.[6−8] Aurora-A is overexpressed in a wide range of human tumors including breast, colorectal, ovarian, and glioma.[9−12] In addition, Aurora-A can transform cells when ectopically expressed in vitro.[10,13] Aurora-B is also overexpressed in human malignancies such as glioma, thyroid carcinoma, seminoma, and colorectal cancer.[14−16] Moreover, exogenous overexpression of Aurora-B (AIM-1) in Chinese hamster embryo cells led to increased levels of phosphorylation of histone H3 at Ser-10 which is associated with chromosome instability and increased tumor invasiveness, indicating a role for Aurora-B in tumor progression.[17] Overexpression of Aurora-C has been observed in some colon cancers;[18] however, its function during mitosis and its involvement in cancer development are less well-defined.

In recent years, the Aurora proteins have been actively pursued as anticancer targets for the discovery of new cancer chemotherapeutics.[19] As a result, several small-molecule inhibitors of Aurora kinases have been identified, some of which have reached clinical evaluation, including **1** (VX-680 (MK-0457)),[20] **2** (PHA-739358),[21,22] **3** (AT9283),[23] **4** (SNS-314),[24] **5** (MLN8054),[25] and **6** (AZD1152)[26] (Figure 1). In clinical trials, these compounds are dosed via the iv administration route, for example, **1**, **2**, **3**, **4**, **6**, or orally, for example, **3**, **5**.[19] The quinazoline derivative **6** has been reported as being a selective Aurora-B inhibitor, whereas **5** is a selective inhibitor of Aurora-A kinase activity. However, in relation to Aurora isoform selectivity, the ideal inhibitor profile for therapeutic use is still unclear.

We have previously reported the identification of the novel imidazo[4,5-*b*]pyridine derivative **7** as a potent inhibitor of Aurora-A (Figure 2).[27,28] Herein, we report our medicinal

‡Atomic coordinates and structure factors for the crystal structures of Aurora-A with compounds **40c** and **51** can be accessed using PDB codes 2X6D and 2X6E, respectively.

*Corresponding authors. (V.B.) Telephone: +44 (0) 20 86438901 ext 4601. E-mail: vassilios.bavetsias@icr.ac.uk. (E.M.) Telephone: +44 (0) 20 87224231. E-mail: Ted.McDonald@icr.ac.uk.

[a]Abbreviations: ADP, adenosine diphosphate; AUC, area under the curve; BOC, *tert*-butoxycarbonyl; dppf, 1,1′-bis(diphenylphosphino)-ferrocene; DIPEA, *N,N*-diisopropylethylamine; DME, 1,2-dimethoxyethane; ESI, electrospray ionization; hERG, the human ether-a-go-go related gene; HPLC, high pressure liquid chromatography, HRMS, high resolution mass spectrometry; INCENP, inner centromere protein; LC, liquid chromatography; LE, ligand efficiency; MLM, mouse liver microsomes; PAMPA, parallel artificial membrane permeability assay; PCy_3, tricyclohexylphosphine; PyBOP, benzotriazol-1-yloxytris(pyrrolidino)-phosphonium hexafluorophosphate; PPB, plasma protein binding; SAR, structure−activity relationship; TFA, trifluoroacetic acid.

Published on Web 06/21/2010

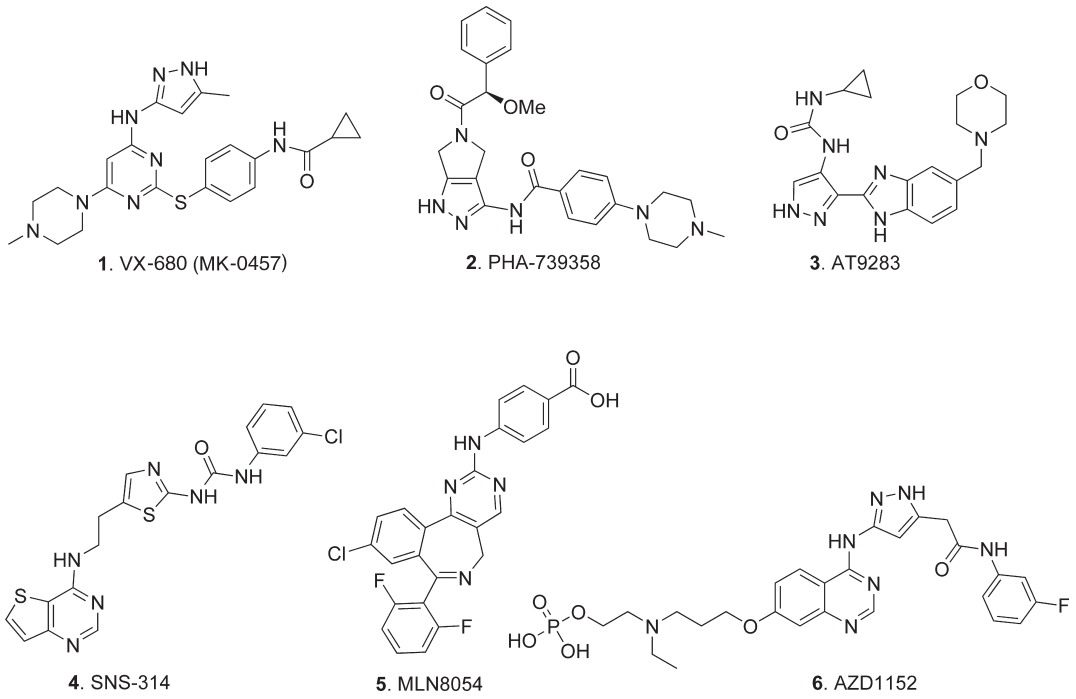

Figure 1. Inhibitors of Aurora kinases.

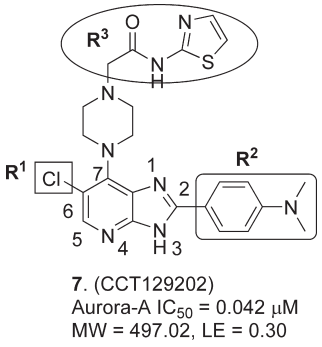

Figure 2. Inhibition of Aurora kinases.[27,28]

chemistry program aimed at converting the potent lead compound **7** to an orally bioavailable inhibitor of Aurora kinases suitable for preclinical evaluation.

Chemistry

The 6-Br derivative **15** was prepared as shown in Scheme 1. The synthesis starts with **8** which was converted to **9** by reacting with *N*-bromosuccinimide in acetonitrile. Nitration of **9** was effected with the use of conc. H_2SO_4/70% HNO_3, and access to the key intermediate **13** was readily gained via an S_NAr substitution reaction on **11**. Formation of **15** from **13** and 4-(dimethylamino)benzaldehyde was accomplished in one step using sodium dithionite ($Na_2S_2O_4$) in ethanol.[29] Starting from **10** which was prepared as previously reported,[30] access to **7** was achieved in a manner similar to its 6-Br counterpart (Scheme 1). The 6-CN derivative **16** (Table 1) was obtained from **15** via a Pd-catalyzed cyanation reaction using $Zn(CN)_2$ as the cyanide source (Scheme 1).

The 6-cyclopropyl analogue **21** (Table 1) was prepared as shown in Scheme 2. Commencing with **11**, access to the BOC-piperazine derivative **17** was achieved via an S_NAr substitution reaction. The 5-cyclopropyl subsituted pyridine derivative **18** was obtained by reaction of **17** with cyclopropylboronic acid

Scheme 1[a]

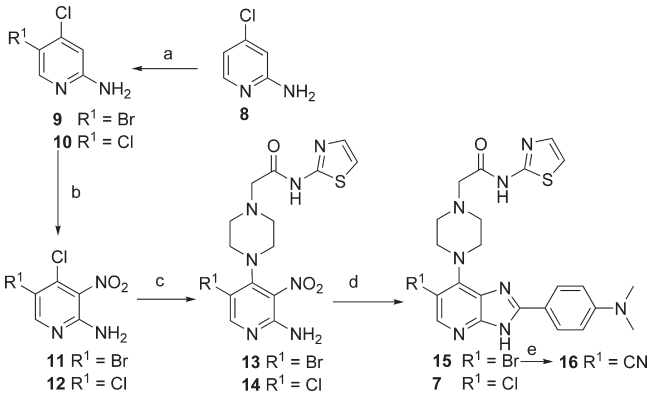

[a] Reagents and conditions: (a) NBS, CH_3CN, 16 h; (b) conc. H_2SO_4, 70% HNO_3, heating, (c) 2-(piperazin-1-yl)-*N*-(thiazol-2-yl)acetamide × 2HCl salt, DIPEA, ^{i}PrOH, overnight; (d) EtOH, 1 M aq. $Na_2S_2O_4$, 4-(dimethylamino)benzaldehyde, 80 °C; (e) DMF, Pd_2dba_3, dppf, $Zn(CN)_2$, μW, 180 °C, 30 min.

under Pd-catalyzed conditions[31] and was then converted to **20** by first removing the BOC group and then reacting **19** with 2-chloro-*N*-(thiazol-2-yl)acetamide. Finally, **21** was obtained from **20** by treatment with *p*-methoxybenzaldehyde in the presence of $Na_2S_2O_4$ in ethanol (Scheme 2).

Access to the R^2 unsubstituted analogue **23** (Figure 2, Table 2) was gained by reducing the nitro group of 2-amino-3-nitropyridine derivative **13** with $Na_2S_2O_4$ in ethanol, followed by ring formation which was achieved using trimethyl orthoformate under acidic conditions (Scheme 3). Analogue **25** (Table 2) was prepared by reacting **13** with *tert*-butyl 4-formylbenzylcarbamate in the presence of $Na_2S_2O_4$ to effect ring formation, followed by TFA removal of the BOC group and dimethylation of the resulting primary amine by treatment with 38% aq. formaldehyde and $NaBH_3CN$ (Scheme 3). Compounds **26**, **27**, and **28** (Table 2) were prepared from **13** or **14** by reacting with

Table 1. R^1 Modifications[a]

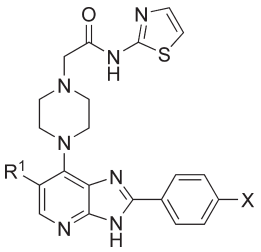

compound	R^1	X	Aurora-A, IC_{50} (μM)	HCT116 GI_{50} (μM)
7	Cl	NMe_2	0.042 ± 0.022^c	0.35^c
15	Br	NMe_2	0.055 ± 0.009	0.48
16	CN	NMe_2	0.050 ± 0.020	1.03^b
21	cyclopropyl	OMe	0.053^b	2.50

[a] Results are mean values of two independent determinations or mean (±SD) for $n > 2$ unless specified otherwise. [b] Results are mean values for samples run in triplicate. [c] From refs 27 and 28.

Scheme 2[a]

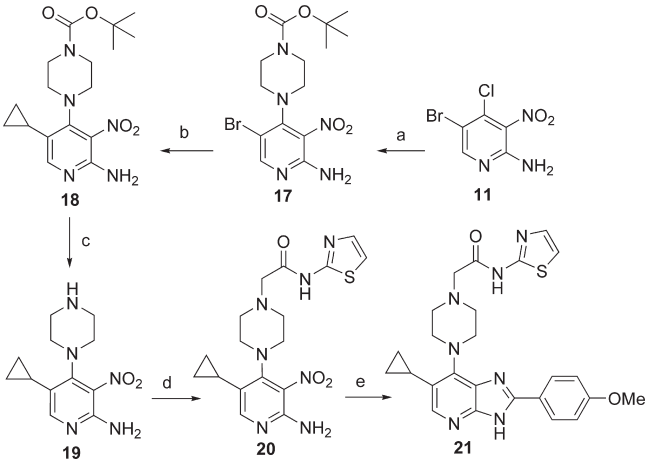

[a] Reagents and conditions: (a) 1-BOC-piperazine, DIPEA, ^{i}PrOH, 45 °C, 20 h; (b) cyclopropylboronic acid, DME, $Pd(OAc)_2$, PCy_3, K_3PO_4, μW, 150 °C, 45 min; (c) TFA,CH_2Cl_2; (d) 2-chloro-*N*-(thiazol-2-yl)acetamide, CH_2Cl_2, DIPEA; (e) EtOH/DMF, 4-methoxybenzaldehyde, 1 M aq. $Na_2S_2O_4$, 80 °C.

the appropriate aldehyde in the presence of $Na_2S_2O_4$ as described for the synthesis of **15** (Scheme 1).

Compound **31a** (Table 3) was obtained from intermediate **17** by treatment with 4-(dimethylamino)benzaldehyde and $Na_2S_2O_4$ in ethanol followed by TFA removal of the BOC protecting group (Scheme 4). Other compounds in Table 3 were readily prepared by reaction of the appropriate 2-amino-3-nitropyridine intermediate **30b−l** with 4-(dimethylamino)-benzaldehyde under standard ring formation conditions (1 M aq. $Na_2S_2O_4$, EtOH or DMF, heating; see Scheme 4). 2-Amino-3-nitropyridine derivatives **30b−d, 30 g−l** were obtained via an S_NAr substitution reaction on **11** or **12** (Scheme 4). Starting from **17**, access to 2-amino-3-nitropyridine derivatives **30e** and **30f** was achieved by first removing the BOC group with TFA followed by treatment with phenyl isocyanate and benzenesulfonyl chloride, respectively (Scheme 4, Table 3).

Piperazines **29b−d**, **29g−l** (Scheme 4) were commercially available with the exception of **29d** and **29i** which were synthesized as shown in Scheme 5. The former was accessed by reaction of the acetic acid derivative **32** with 3-chloroaniline under standard amide bond formation conditions (benzotriazol-1-yloxytris(pyrrolidino)phosphonium hexafluorophosphate, DIPEA, CH_2Cl_2) followed by protecting group cleavage. The latter was obtained from 1-(pyridin-4-yl)ethanol[32] by treatment with MsCl in the presence of triethylamine followed by mesylate displacement with 1-BOC-piperazine, and finally removal of the BOC protecting group with TFA.

Synthesis of the 4-methoxyphenyl and morpholinomethylphenyl analogues **39a−h** and **40a−h** (Table 4) is shown in Scheme 6 and was accomplished in a manner similar to the dimethylaminophenyl series (Schemes 4 and 6). The key intermediates **38a−h** were obtained by a nucleophilic displacement of the C-4 chloride of **11** with the requisite piperazine (Scheme 6). Piperazines **37a**, **37c**, and **37d** were commercially available; **37b** and **37g** were prepared by a reductive amination of the corresponding aldehyde with 1-BOC-piperazine followed by removal of the BOC protecting group (Scheme 7).

The piperazine derivatives **37e**, **37f**, and **37h** were obtained via a substitution reaction on the appropriate heteroarylmethyl halide followed by the removal of the BOC protecting group (Scheme 8, Table 4).

Compounds listed in Table 6 were prepared by treating **38e** or its 5-chloro counterpart with the required benzaldehyde in the presence of $Na_2S_2O_4$. For the synthesis of **44**, **46**, **47**, and **50**, the amino functionality present on the requisite benzaldehyde was protected with the BOC group which was removed with TFA after ring formation. Compound **45** was obtained from **46** by a reductive alkylation reaction (38% aq. formaldehyde, THF/MeOH, $NaBH_3CN$).

Results and Discussion

As previously reported, compound **7** inhibits Aurora-A, -B, and -C with IC_{50} values of 0.042, 0.198, and 0.227 μM, respectively,[27] and is also potent in inhibiting cell proliferation in a range of cancer cell lines.[28] Additionally, compound **7** displayed selectivity for inhibition of Aurora-A and Aurora-B proteins in a small kinase panel.[28] Regarding the binding mode of **7** to Aurora-A, we had no crystallographic data on **7** or a closely related analogue bound to Aurora-A when we initiated the lead optimization process. However, the SAR data obtained during the hit-to-lead exploration program[27] and modeling studies suggested that the pyridine N and imidazole NH form hydrogen bonds to Ala213 in the hinge region of Aurora-A with the 2-dimethylaminophenyl substituent pointing to the solvent accessible area. The imidazole NH in 2-arylimidazo-[4.5-*b*]pyridines is a strong hydrogen donor, and the pK_a value of the imidazole NH in 2-phenylimidazo[4.5-*b*]pyridine was reported as 11.07.[33] The hit-to-lead exploration chemistry also suggested that substitution at the 6-position was sterically limited; however, compound **7** was a considerably more potent inhibitor of Aurora-A compared with the 6-unsubstituted counterpart.[27] We had no clear understanding of the interactions of the (piperazin-1-yl)-*N*-(thiazol-2-yl)acetamide moiety in **7** with the protein. With this in mind, we decided to explore in more detail the role of the R^3 substituent (Figure 2) in relation to Aurora-A kinase activity. By modifying the R^3 substituent, we were also aiming to reduce the molecular weight and remove the 2-aminothiazole moiety, a potential toxicophore.[34,35] Our second objective was to replace the R^2 dimethylaminophenyl moiety because of the known toxicity liabilities associated with aniline derivatives.[35,36] Finally, we were planning to optimize the C-6 position within the steric

Table 2. R^2 Modifications[#]

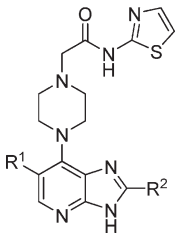

Compound	R^1	R^2	Aurora-A, IC_{50} (μM)	HCT116 GI_{50} (μM)
7	Cl	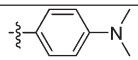	0.042±0.022[b]	0.35[b]
15	Br	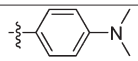	0.055±0.009	0.48
23	Br	H	0.517±0.183	40% at 10μM
25	Br	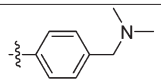	0.016±0.005	1.0[a]
26	Br		0.081±0.043	3.0[a]
27	Cl	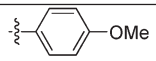	0.052±0.048	0.9
28	Cl	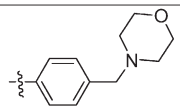	0.003[a]	0.36[a]

[#] Results are mean values of two independent determinations or mean (±SD) for $n > 2$ unless specified otherwise. [a] Results are mean values for samples run in triplicate. [b] From refs 27 and 28.

Scheme 3[a]

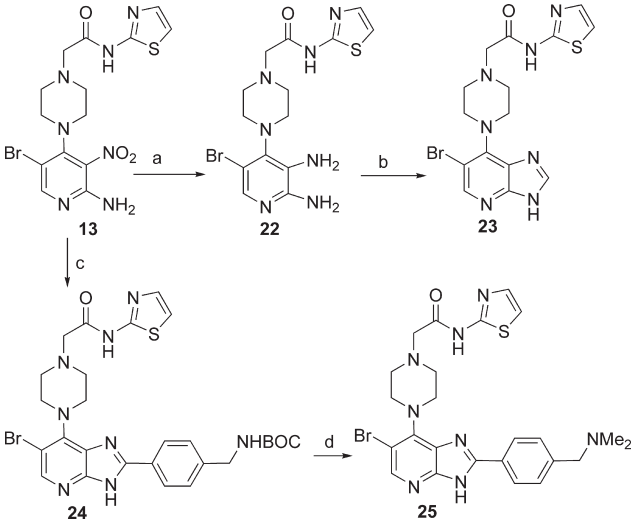

[a] Reagents and conditions: (a) EtOH, 1 M aq. $Na_2S_2O_4$, 80 °C, 16 h; (b) $(MeO)_3CH$, conc. HCl, room temp., 24 h; (c) *tert*-butyl 4-formylbenzylcarbamate, EtOH, 1 M aq. $Na_2S_2O_4$, 80 °C; (d) i. TFA/CH_2Cl_2, ii. 38% aq. formaldehyde, THF/MeOH, $NaBH_3CN$.

constraints already determined by our previous work. To this end, a limited exploration of the R^1 substituent was undertaken, and it was found that Br is well tolerated, compound **15** displaying Aurora IC_{50} and HCT116 GI_{50} (50% cell growth inhibitory concentration) values similar to those of **7** (Table 1). The 6-CN and 6-cyclopropyl derivatives **16** and **21**, respectively, (Table 1) inhibited in vitro Aurora-A kinase activity equivalent to **7** and **27** but were less potent in inhibiting HCT116 cell growth relative to their 6-Cl counterparts **7** (Table 1) and **27** (Table 2).

Subsequently, our chemical effort was focused on the R^2 substituent (Figure 2, Table 2). Removal of the dimethylamino group in **15** did not significantly change the Aurora-A inhibitory activity (compound **15** versus **26**; Table 2), but the replacement of the 2-aryl substituent in **15** with a proton led to a ~10-fold drop in potency against Aurora-A (compounds **23**, **15**; Table 2), indicating that the phenyl ring plays an important role in binding to the Aurora-A kinase and consequent translation to cell based antiproliferative activity. Next, the NMe_2 moiety in **7** or **15** was replaced with a methoxy, dimethylaminomethyl, and a morpholinomethyl group (compounds **27**, **25**, and **28**; Table 2), with all three analogues demonstrating cellular potencies comparable to those of **7** or **15**. Interestingly, inhibitory activity against the Aurora-A enzyme was retained or significantly improved, with **28** being ~10-fold more potent inhibitor compared with **7** (Table 2). These results were very encouraging and clearly demonstrated that the dimethylaminophenyl moiety, a potential toxicophore, could be replaced with retention or an enhancement of the Aurora-A inhibitory activity without compromising the cellular potency.

Table 3. R^3 Modifications[#]

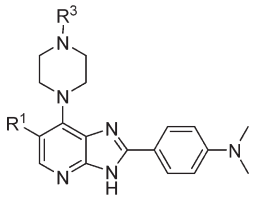

Compound	R^1	R^3	Aurora-A, IC_{50} (μM)	HCT116 GI_{50} (μM)
7	Cl	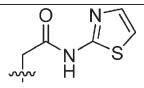	0.042±0.022[b]	0.35[b]
15	Br	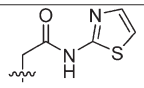	0.055±0.009	0.48
31a	Br	H	0.365	0.95[a]
31b	Cl	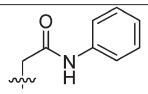	0.115	2.55[a]
31c	Br	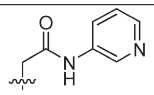	0.118	1.65
31d	Cl	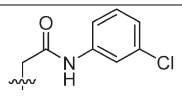	0.075	2.67[a]
31e	Br	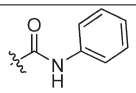	0.277 ±0.071	10.0[a]
31f	Br		0.178[a]	n.d.[c]
31g	Br		0.258[a]	n.d.[c]
31h	Br		0.210	0.97
31i	Br	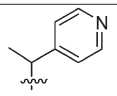	0.085	0.90
31k	Cl	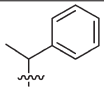	0.079	0.90
31l	Br		0.055	0.70[a]

[#] Results are mean values of two independent determinations or mean (±SD) for $n > 2$ unless specified otherwise. [a] Results are mean values for samples run in triplicate. [b] From refs 27 and 28. [c] n.d. = not determined.

To evaluate the contribution of the undesirable *N*-(thiazol-2-yl)acetamide moiety to the inhibitory potency of **7** or **15**, we prepared the unsubstituted compound **31a** (Table 3). This analogue was ~8-fold less potent in inhibiting the Aurora-A kinase compared with the parent **15**. The replacement of the thiazole ring in **15** or **7** with a phenyl, pyridyl, or a substituted phenyl (compounds **31b**, **31c**, and **31d**, respectively) was broadly tolerated, but all three compounds were less potent inhibitors of the HCT116 cell growth relative to **15** or **7** (Table 3). The attachment of a phenyl group to the piperazine

Scheme 4[a]

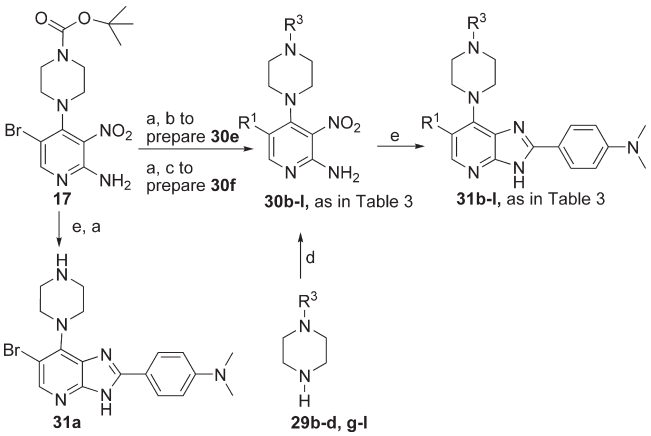

[a] Reagents and conditions: (a) TFA/CH_2Cl_2; (b) $CHCl_3$, DIPEA, PhNCO, room temp., 12 h; (c) $CHCl_3$, pyridine, $PhSO_2Cl$, room temp., 12 h; (d) 2-amino-4,5-dichloro-3-nitropyridine or 2-amino-5-bromo-4-chloro-3-nitropyridine, DIPEA, ^{i}PrOH, heating; (e) 4-(dimethylamino)-benzaldehyde, EtOH or DMF, 1 M aq. $Na_2S_2O_4$, 80 °C.

Scheme 5[a]

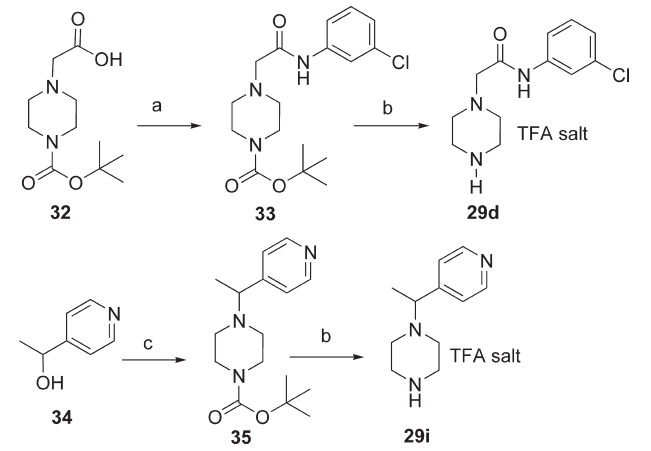

[a] Reagents and conditions: (a) 3-chloroaniline, benzotriazol-1-yloxytris-(pyrrolidino)phosphonium hexafluorophosphate, DIPEA, CH_2Cl_2; (b) TFA/CH_2Cl_2; (c) i. MsCl, Et_3N, CH_2Cl_2, ii. 1-BOC-piperazine, DMSO, 60 °C, 18 h.

ring, directly or via an amide or a sulphonyl linker, had a detrimental effect on enzyme inhibition (compounds **31g**, **31e**, and **31f**; Table 3). Likewise, the isobutyl derivative **31h** was a weaker inhibitor of Aurora-A (IC_{50} value of 0.210 μM compared with that of 0.055 μM for **15**). However, the attachment of a phenyl or a 4-pyridyl group to the piperazine ring via a $CH(CH_3)$ linker (compounds **31k** and **31i**, respectively; Table 3) was well tolerated regarding both Aurora-A enzyme inhibition and HCT116 cellular potency. Compounds **31i** and **31k** inhibited Aurora-A with IC_{50} values of 0.085 and 0.079 μM, respectively, prompting the introduction of the pyridin-4-ylmethyl group as the R^3-substituent (**31l**, Table 3). Compound **31l** was a potent inhibitor of both the Aurora-A kinase activity and the HCT116 cell growth, with IC_{50}/GI_{50} values of 0.055 and 0.70 μM, respectively. Subsequent combination of R^1 = Cl, R^2 = *p*-methoxyphenyl, and R^3 = pyridin-4-ylmethyl led to compound **36a** (Figure 3), a potent Aurora-A inhibitor (IC_{50} = 0.021 μM) devoid of the toxicophore liabilities associated with **7**, and of lower molecular weight and higher ligand efficiency compared with **7** (Figure 3). On

Table 4. R^3 Benzyl Replacement[#]

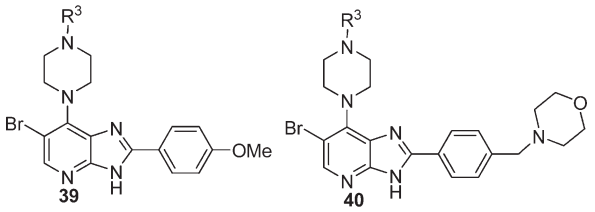

Compound	R^3	Aurora-A, IC_{50} (μM)	HCT116 GI_{50} (μM)
39a		0.009	1.15
40a		0.005± 0.004	0.28
39b		0.008[a]	0.40[a]
40b		0.006	0.42[a]
39c	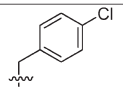	0.040[a]	0.36[a]
40c		0.012	0.60±0.06
39d		0.65[a]	0.83[a]
39e	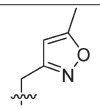	0.017[a]	0.54±0.30
40e		0.002	0.06
39f	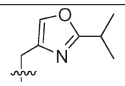	0.081[a]	0.40[a]
39g		0.032[a]	1.5[a]
40g		0.030[a]	1.5[a]
39h		0.004[a]	0.32[a]
40h		0.006[a]	n.d.[c]

[#] Results are mean values of two independent determinations or mean (±SD) for $n > 2$ unless specified otherwise. [a] Results are mean values for samples run in triplicate. [c] n.d. = not determined.

this basis, **36a** (Figure 3) was selected as a scaffold to identify the substituents with optimum in vitro profile and evaluate the most promising compounds for kinase selectivity and in vivo PK properties. The 6-Br counterpart of **36a** (compound **36b**) was also prepared and displayed a similar Aurora-A inhibitory potency (IC_{50} = 0.015 μM). Optimization of the R^3 benzyl group was carried out with a 6-Br substituent due to availability of bulk intermediate, while the neutral *p*-methoxyphenyl group and the weakly basic morpholinobenzyl moiety were utilized as the R^2 substituents (Figure 3, Table 4).

In the R^2 = *p*-methoxyphenyl series (compounds **39a**−**h**), the introduction of 3-pyridyl or a pyrimidinyl ring was beneficial versus inhibition of Aurora-A kinase (compound **39a**, IC_{50} = 0.009 μM; compound **39b**, IC_{50} = 0.008 μM). The pyrimidinyl derivative **39b** exhibited higher cellular potency relative to **39a**, but lower stability in mouse liver microsomes (35% of parent compound remaining after 30 min incubation). The introduction of the *p*-chlorophenyl group provided no Aurora-A inhibitory benefit (**39c**, IC_{50} = 0.040 μM) but **39c**

Scheme 6[a]

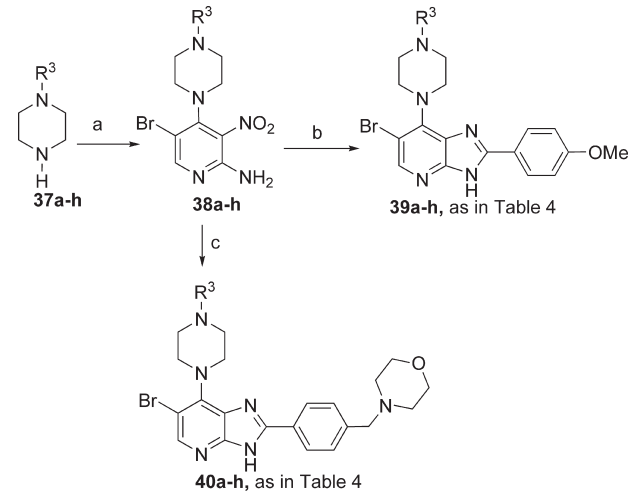

[a] Reagents and conditions: (a) 2-amino-5-bromo-4-chloro-3-nitropyridine, DIPEA, ^{i}PrOH, heating; (b) 4-methoxybenzaldehyde, EtOH, 1 M aq. $Na_2S_2O_4$, 80 °C; (c) 4-(morpholinomethyl)benzaldehyde, EtOH, 1 M aq. $Na_2S_2O_4$, 80 °C.

Scheme 7[a]

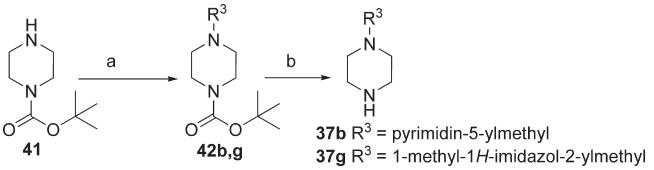

[a] Reagents and conditions: (a) pyrimidine 5-carboxaldehyde, $NaBH_3CN$, EtOH, AcOH, or 1-methyl-1*H*-imidazole-2-carbaldehyde, 1,2-dichloroethane, $NaBH(OAc)_3$; (b) TFA/CH_2Cl_2.

Scheme 8[a]

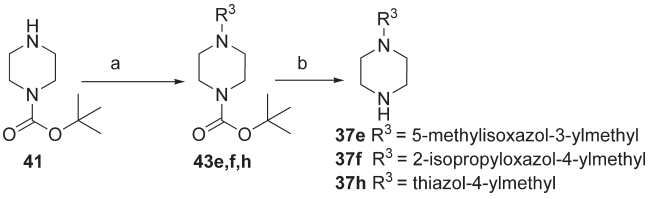

[a] Reagents and conditions: (a) 3-bromomethyl-5-methylisoxazole, CH_2Cl_2 or 4-(chloromethyl)-2-isopropyloxazole, DIPEA, CH_2Cl_2 or 4-(chloromethyl)thiazole, DIPEA, CH_2Cl_2; (b) TFA/CH_2Cl_2.

was potent in cells (GI_{50} = 0.36 μM). The cyclopropylmethyl analogue **39d** followed the same trend seen with the isobutyl derivative **31h** (Table 3), namely, inferior inhibition of Aurora-A (IC_{50} = 0.65 μM) but relatively potent in HCT116 cells (GI_{50} = 0.83 μM). Subsequently, a range of 5-membered ring aromatic heterocycles was explored. The introduction of the 5-methylisoxazole (**39e**, Table 4) was well tolerated. Compound **39e** was a potent inhibitor of the Aurora-A kinase and the HCT116 cell growth (IC_{50} = 0.017, GI_{50} = 0.54 μM) with good stability in mouse liver microsomes (>50% remaining after 30 min incubation). The isopropyloxazole analogue **39f** was relatively inferior on inhibiting the kinase (IC_{50} = 0.081 μM), and metabolically labile (only 11% remaining after 30 min incubation with mouse liver microsomes). The *N*-methylimidazole derivative **39g** displayed inferior cellular potency (GI_{50} = 1.5 μM), and the thiazole analogue **39h** suffered from a moderate stability in mouse liver microsomes (45% remaining after a 30 min incubation). In the R^2 morpholinobenzyl series (compounds **40a−h**), the effect of the R^3 substituent followed a similar trend with that observed in the R^2 = *p*-methoxyphenyl series (compounds **39a−h**, Table 4) with two notable exceptions. In line with observations in the R^3 = *N*-(thiazol-2-yl)acetamide series (Table 2), the morpholinomethyl group appeared to have a higher affinity for the enzyme as demonstrated with compounds **40c** (CCT137444) and **40e** (Table 4). However, the morpholinomethyl derivatives exhibit lower stability in mouse liver microsomes, probably a reflection of metabolic liabilities associated with the morpholine ring.[37]

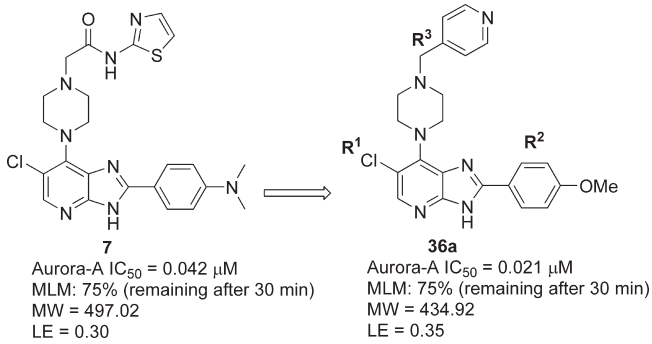

Figure 3. A new class of imidazo[4,5-*b*]pyridine-based inhibitors of Aurora kinases.

Table 5. Kinase Selectivity Profile of **40c**

kinase	% inhibition at 1 μM
Aurora-B	60
EPHB4	4
FLT1 (VEGFR1)	35
KDR (VEGFR2)	35
LCK	8
MET (cMET)	3
NTRK1 (TRKA)	33
PDGFR beta	15
Aurora-A	98
TEK (Tie2)	5

To obtain an indication of the kinase selectivity for this class of imidazo[4,5-*b*]pyridine-based inhibitors of Aurora kinases, **40c** was evaluated in a panel of 10 kinases. At a compound concentration of 1 μM, it was found that **40c** inhibited only Aurora-A and Aurora-B to a significant level (Table 5). For selected examples, affinity for the hERG ion-channel was determined. Compound **39e** had no effect on hERG tail-currents, but **40c** was a weak inhibitor of hERG (53% inhibition at 10 μM).

To determine the binding mode of this class of inhibitors, we cocrystallized the catalytic domain of Aurora-A (residues 122−403) with **40c**. The crystal structure of compound **40c** bound to Aurora-A (determined to a resolution of 2.8 Å, Figure 4A, Table S1 in Supporting Information) confirmed our hypothesis that the pyridine N and imidazole NH are interacting with Ala213 in the hinge region of the kinase. Compound **40c** occupies the ATP-binding site with the activation loop in a DFG-in conformation. The pyridine N is hydrogen bonded to backbone NH of Ala213 (2.9 Å) and the imidazole NH to the carbonyl of Ala213 (2.9 Å) as shown in Figure 4. The 6-Br substituent occupies a small lipophilic pocket defined by the side chains of Val147, Ala160, Leu194, and Leu210 (4−4.2 Å distant). The morpholinomethylphenyl substituent points to the solvent accessible area with the

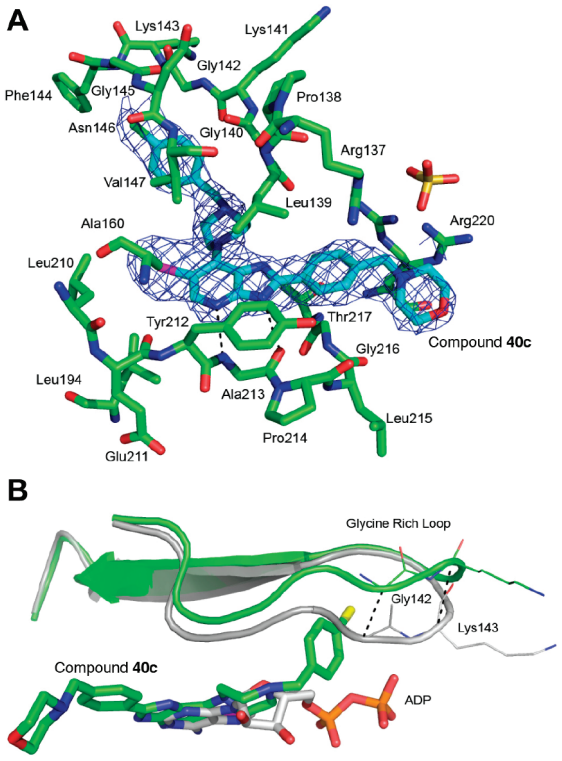

Figure 4. 2.8 Å resolution crystal structure of compound **40c** bound to Aurora-A. (A) Stick representation of **40c** (carbon atoms colored cyan) bound to Aurora-A (carbon atoms colored green) with the final $F_o - F_c$ electron density map contoured at 1.0σ shown as a wiremesh. (B) Cartoon representation of the Gly-rich loop and stick representation of ligand in ADP-bound Aurora-A (gray cartoon and carbon atoms) and **40c**-bound Aurora-A (green cartoon and carbon atoms).

phenyl ring residing at close proximity to Gly216. The R^3 *p*-chlorobenzyl substituent interacts with the Aurora-A kinase Gly-rich loop at the backbone of residues Gly140, Lys141, and Asn146. This interaction induces an approximately 3 Å outward conformational shift of the Gly-rich loop with respect to the conformation observed in the ADP-bound form of Aurora-A (Figure 4B).

Subsequently, on the basis of desirable in vitro properties, a set of compounds was selected for in vivo PK profiling. Oral bioavailability was 13% and 23% for compounds **40a** and **39e**, respectively. Though permeability, determined as 6×10^{-6} cm/s for **39e** in the PAMPA assay (pH6.5), was not excluded as the cause of the low bioavailability, this was mainly attributed to low aqueous solubility (measured as 0.03 mg/mL for **40a**, and < 0.01 mg/mL for **39e**). These findings suggest that although potent inhibitors of Aurora kinases with desirable cellular potency and mouse liver microsomal stability have been identified, their physicochemical properties and in particular solubility may limit their utility. Consequently, solubility-enhancing features such as alcohols, heterocycles, and basic amines were designed in the subsequent compound set. We sought to introduce such groups at the *p*-position of the R^2 phenyl substituent (Table 6) with the aim of simultaneously maintaining or improving the kinase inhibitory activity. Our ultimate objective was to identify compounds for in vivo PK characterization and in vivo efficacy studies. To achieve this, we mainly focused our chemical efforts on three R^3 substituents: *p*-chlorobenzyl, 5-methylisoxazol-3-ylmethyl, and pyridin-3-ylmethyl (based on the in vitro compound profiling). Particular attention was given to R^3 5-methylisoxazol-3-ylmethyl since the 5-methylisoxazole moiety has the lowest contribution to overall compound cLogP (0.39) relative to pyridine (0.65) and chlorobenzene (2.86).[38] The results for the 5-methylisoxazole derivatives are shown in Table 6.

Table 6. Incorporation of Solubilizing Groups[#]

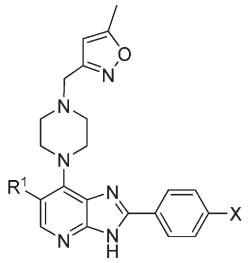

Compound	R^1	X	Aurora-A, IC_{50} (μM)	HCT116 GI_{50} (μM)
44	Br	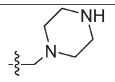	0.010	0.078
45	Br	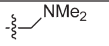	0.014	0.23 ±0.07
46	Br	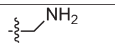	0.010[a]	0.24[a]
47	Cl	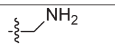	0.055	0.65
48	Br	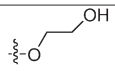	0.030[a]	0.28[a]
49	Cl	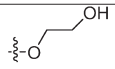	0.029	0.45
50	Br	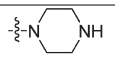	0.010[a]	0.10
51	Br	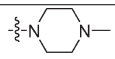	0.015±0.003	0.35±0.18
52	Cl	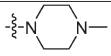	0.010	0.14[a]
53	Br	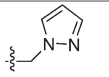	0.003	0.12[a]
54	Cl	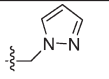	0.010[a]	0.45

[#] Results are mean values of two independent determinations or mean (±SD) for $n > 2$ unless specified otherwise. [a] Results are mean values for samples run in triplicate.

For selected examples, aqueous solubility was obtained; it was found that X substituents bearing a basic nitrogen fulfilled our expectations. For example, the aqueous solubility for compounds **44** and **51** (CCT137690) was determined as 0.87 mg/mL and 0.23 mg/mL, respectively. On the other hand, no benefit was gained from the introduction of the hydroxyethoxy moiety as a solubilizing group; the measured solubility for compound **48** was low (0.01 mg/mL). The vast majority of the synthesized analogues were potent inhibitors of Aurora-A and of HCT116 cell growth (Table 6). In addition, compounds **44**−**52** displayed good stability in mouse liver microsomes (> 50% of parent compound remaining after

30 min incubation). This desirable set of in vitro properties (i.e., enzymatic/cellular potency, and mouse liver microsomal stability) justified the in vivo PK characterization for many of compounds shown in Table 6. A selection of compounds including the piperazinyl derivative **44** (Table 6) were administered iv in a cassette of five compounds for PK profiling. Pharmacokinetic analysis indicated a rapid plasma clearance for **44** with undetectable levels 1 h postadministration of 1 mg/kg. To further accelerate the compound PK profiling, suitable analogues (compounds **45**−**52**, Table 6) were first subjected to a "limited PK" evaluation in which plasma and muscle (as a surrogate for tumor) compound concentrations were determined at 6 and 24 h following oral administration to mice (dose of 5 mg/kg). The hydroxyethoxy derivative **49** and the benzylamine derivative **47** were only detected at the 6 h time point in plasma at a total concentration < 10 nM and not in muscle. Likewise, the *N,N*-dimethylbenzylamine analogue **45** was only detected at 6 h post dose in plasma (total concentration = 90 nM). In contrast, compound **51** was detectable in both plasma and muscle at the 6 h time point (total concentration in plasma = 250 nM). Compound **52** was present in both plasma and muscle at 6 h post dose at levels similar to those determined for **51**. However, **52** was not detectable in muscle at 24 h, whereas **51** was present in muscle at 24 h (total concentration = 10 nM). Assuming linear pharmacokinetics, the compound concentration at the two time points (6, 24 h) was projected based upon an oral dose of 50 or 100 mg/kg. Calculated values significantly above the compound cellular GI_{50} value led to further investigation of the full in vivo PK. By following these experimental triage procedures, compound **51** was identified having the optimal combination of in vitro and in vivo properties. It is a completely orally bioavailable inhibitor (F = 100%) of Aurora kinases with desirable pharmacokinetic parameters in mouse (Cl: 0.037 L/h (~25 mL/min/kg), Vd: 0.087 L (~3.5 L/kg); Table 7).

Table 7. Compound **51**: Mouse Plasma Protein Binding, and PK Parameters in Mouse (iv dosing: 1 mg/kg)

PPB (mouse)	$t_{1/2}$, (iv) (h)	Cl (L/h)	AUC, (iv) h·nmol/L	Vd (L)	F% (po)
98.0 ± 0.5	1.6	0.037	994	0.087	100

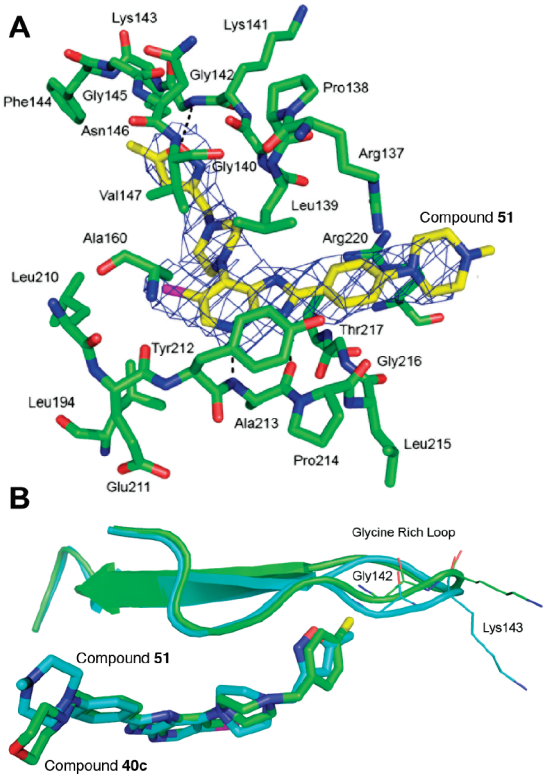

Figure 5. 3.35 Å resolution crystal structure of **51** bound to Aurora-A. (A) Stick representation of **51** (carbon atoms colored yellow) bound to Aurora-A (carbon atoms colored green) with the final $F_o - F_c$ electron density map contoured at 1.0σ shown as a wiremesh. (B) Cartoon representation of the Gly-rich loop and stick representation of ligand in **51**-bound Aurora-A (cyan cartoon and carbon atoms) and **40c**-bound Aurora-A (green cartoon and carbon atoms).

Compound **51** was profiled in a 94-kinase panel, and at a concentration of 1 μM, inhibited only three kinases at a level higher than 80%, that is, Aurora-A, FGF-R1, and VEG-FR (see Table S2 in Supporting Information).

Compound **51** inhibited Aurora-B and Aurora-C with IC_{50} values of 0.025 and 0.019 μM, respectively, and displayed antiproliferative activity in a range of human tumor cell lines, including SW620 colon carcinoma (GI_{50} = 0.30 μM) and A2780 ovarian cancer cell line (GI_{50} = 0.14 μM). In addition, **51** inhibited in vitro the phosphorylation of histone H3, a biomarker for inhibition of Aurora-B kinase (data not shown - to be reported elsewhere). Regarding key safety pharmacology parameters, **51** was tested for inhibition of the hERG ion-channel and cytochrome P450 isoforms. It inhibited the major cytochrome P450 isoforms (CYP1A2, CYP2A6, CYP2C9, CYP2C19, CYP2D6, CYP3A4) with an IC_{50} value greater than 10 μM. However, **51** was a moderate inhibitor of

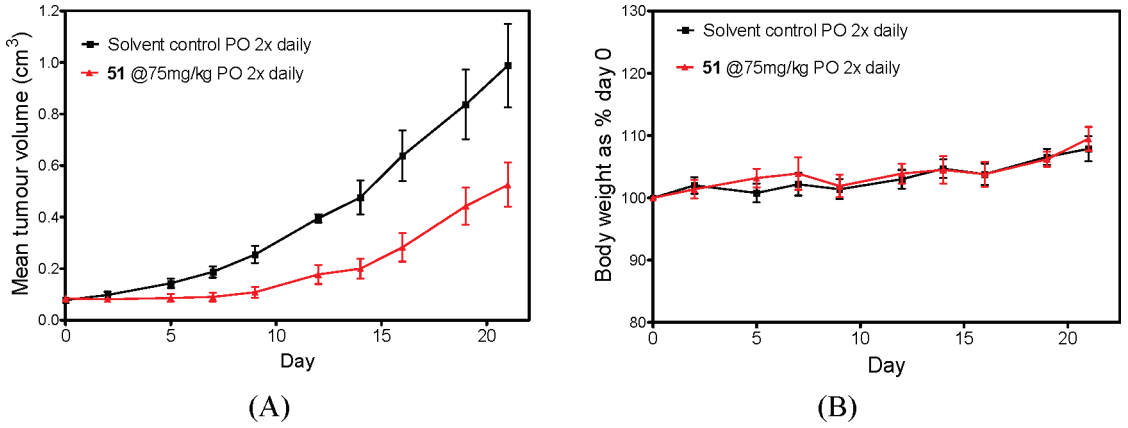

Figure 6. In vivo efficacy of **51** against SW620 human colon carcinoma xenografts in athymic mice. (A) Mean tumor volumes ± SEM, (B) mouse body weights.

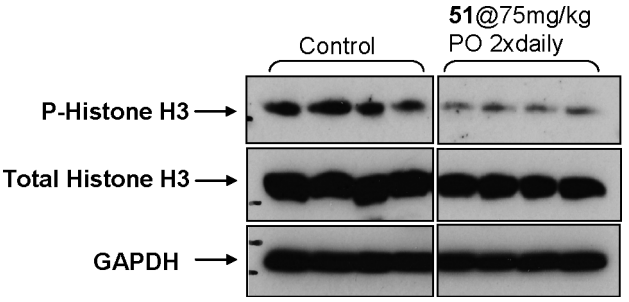

Figure 7. Compound **51** inhibits histone H3 phosphorylation in SW620 xenografts. Tumour samples were obtained 6 h after the final dose and analyzed for histone H3 phosphorylation. Total histone H3 and GAPDH were used as loading controls.

the hERG ion-channel (IC_{50} = 3.0 μM; n = 2). The 6-Cl counterpart of **51**, compound **52** (Table 6), displayed a similar hERG inhibitory activity (IC_{50} = 2.3 μM).

The crystal structure of **51** bound to Aurora-A was determined to a resolution of 3.35 Å, and shows that **51** occupies the ATP-binding site in a binding mode similar to that described for **40c** (Figure 5A). Compound **51** makes contacts with the Gly-rich loop that are similar to that observed for **40c**, the isoxazole O and N have the potential to act as H-bond acceptors, and in our model the O sits 3.1 Å away from the backbone NH of Gly142. However, the resolution of this structure is insufficient to determine whether H-bonding occurs between the isoxazole and Aurora-A. Compound **51** induces a similar conformational shift in the Gly-rich loop as **40c** (Figure 5B).

On the basis of the encouraging PK parameters of **51**, the absence of concerns related to inhibition of P450 isoforms, desirable Aurora-A enzyme/cellular potency, and pharmacodynamic effect related to inhibition of Aurora kinases, **51** was evaluated in in vivo efficacy studies (Figure 6). Athymic mice bearing established SW620 human colorectal tumors were treated with either vehicle (DMSO-Tween-saline) or **51** administered orally at a dose of 75 mg/kg twice a day for 21 days. Compound **51** slowed the growth of the SW620 xenografts with no observed toxicity as defined by body weight loss (Figure 6B). The treated/control (T/C) ratio was calculated as 42.4% based on final tumor weights (not shown). A repeat efficacy study with **51** (75 mg/kg p.o. twice daily for 17 days) showed comparable efficacy (T/C = 37%), and inhibition of histone H3 phosphorylation, a biomarker for Aurora-B kinase inhibition (Figure 7). These findings are consistent with target modulation in vivo by compound **51**.

Conclusion

In the course of this work, our goal was to convert **7** to an orally bioavailable inhibitor of Aurora kinases suitable for preclinical evaluation. This led to a new class of imidazo[4,5-*b*]-pyridine-based inhibitors of Aurora kinases possessing the 1-benzylpiperazinyl motif at the 7-position. Compounds belonging to this class are devoid of the potential toxicophore liabilities associated with **7**, and a significant number of analogues displayed favorable in vitro properties (enzymatic/cellular potency, and mouse liver microsomal stability). Cocrystallization of Aurora-A with **40c** bound provided a clear understanding of the interactions of this novel class of inhibitors with the Aurora-A kinase. Subsequent physicochemical property refinement by reduction of lipophilicity and the introduction of solubilizing groups led to the identification of **51** which is a highly orally bioavailable and potent inhibitor of Aurora kinases. In an in vivo efficacy evaluation, **51** inhibited the growth of SW620 colon cancer cell xenografts following oral administration with no observed toxicities as defined by body weight loss. However, **51** has a narrow safety margin against hERG which may limit its preclinical development and the discovery of compounds with a wider therapeutic index versus hERG will be the subject of future publications.

Experimental Section

Aurora Kinase Assays. Aurora kinase IC_{50} values were determined as previously described.[28]

Kinase Selectivity Profiling. Compound **51** was profiled against a panel of 94 kinases at the National Centre for Protein Kinase Profiling, Division of Signal Transduction Therapy, University of Dundee.

Cell Viability Assay. GI_{50} values (50% cell growth inhibitory concentration) were determined as previously described.[28]

Cocrystallization of Aurora-A with Ligand. Wild-type Aurora-A catalytic domain (residues 122−403) was expressed and purified as previously described.[39] Cocrystals with **40c** were produced using Bicine pH 9.0, 2.0 M $(NH_4)_2SO_4$ as crystallization buffer. Cocrystals with **51** were produced using 0.1 M NaCl, 0.1 M HEPES pH 7.5, 1.6 M $(NH_4)_2SO_4$ as crystallization buffer. Crystals were briefly soaked in crystallization buffer supplemented with 25% ethylene glycol **40c** or 30% glycerol **51** before flash freezing in liquid N_2. Structures were solved by molecular replacement using Aurora-A (PDB code 1MQ4) as a model. Ligand fitting and model rebuilding was carried out using Coot,[40] and refinement was carried out using Phenix.[41]

Mouse Liver Microsomal Stability. Compounds (10 μM) were incubated with male CD1 mouse liver microsomes (1 mg mL^{-1}) protein in the presence of NADPH (1 mM), UDPGA (2.5 mM), and $MgCl_2$ (3 mM) in phosphate buffered saline (10 mM) at 37 °C. Incubations were conducted for 0 and 30 min. Control incubations were generated by the omission of NADPH and UDPGA from the incubation reaction. The percentage compound remaining was determined after analysis by LCMS.

Inhibition of Cytochrome P450 Isoforms. Inhibition of human liver CYP isozymes was assessed in human liver microsomes (pool of 50 individuals) as previously described[42] with the following modifications: microsomal protein concentration 0.5 mg/mL, incubation time 10 min, mephenytoin as the CYP2C19 substrate and metabolite detection by LCMSMS ESI+ on a Shimadzu LC system connected to a QTRAP 4000 (Applied Biosystems).

Aqueous Solubility. Compound kinetic aqueous solubility was determined by Evotec, Abingdon, Oxfordshire, UK.

Inhibition of hERG. hERG IC_{50} values were determined by Millipore (Millipore UK Ltd., Cambridge, UK).

In Vivo "Limited PK". All animal studies were performed in accordance with the UK guidelines for animal use and welfare (UKCC). Compounds were formulated at 0.5 mg mL^{-1} in 10% DMSO, 5% Tween 20 in sterile saline. Female Balb/C mice received an oral dose of compound (5 mg/kg). After administration, mice were bled at 6 and 24 h. Blood was removed by cardiac puncture in heparinised syringes and centrifuged to obtain plasma samples for PK analysis. Muscle and liver were harvested for analysis. Plasma samples (50 μL) were extracted by protein precipitation by addition of 150 μL of methanol containing internal standard (IS). Tissue samples were homogenized with 3v/w of PBS and compound extracted from the resulting homogenate as described for plasma. Plasma and homogenate extracts were analyzed by LCMS using reverse-phase Eclipse Plus C18 (Agilent, 50 × 2.1 mm) analytical column and positive ion mode ESI MRM.

Cassette Dose Pharmacokinetic Profiling. Five compounds were formulated at 0.1 mg/mL in 10% DMSO, 5% Tween 20 in

saline. Balb C female mice received the compound mixture via iv administration at 1 mg/kg per compound. Following compound administration, mice were terminated at 0.083, 0.25, 0.5, 1, 2, 4, 6, and 24 h. Blood was removed by cardiac puncture and centrifuged to obtain plasma samples and tissues harvested for PK analysis. Plasma samples (150 μL) were extracted by protein precipitation by addition of 150 μL of acetonitrile containing internal standard (IS). Tissues were homogenized with 3*w*/v of PBS prior to protein precipitation with acetonitrile containing IS. Plasma and tissue extracts were analyzed by LCMS using reverse-phase analytical column and positive ionization mode with multiple reaction monitoring of optimized transitions.

In Vivo Full PK (Compound 51). Full pharmacokinetic analysis was performed at 1 mg/kg (iv) and 5 mg/kg (po) as described in ref 28.

Human Tumor Xenograft Efficacy Study. Procedures involving animals were carried out within guidelines set out by The Institute of Cancer Research's Animal Ethics Committee and in compliance with national guidelines (Workman P., Twentyman P., Balkwill F., et al. United Kingdom Co-ordinating Committee on Cancer Research (UKCCCR) Guidelines for the Welfare of Animals in Experimental Neoplasia (Second Edition). Br J Cancer, 77: 1−10, 1998).

Human SW620 colon carcinoma cells (4×10^6) were injected subcutanously (s.c.) in the right flank of female CrTac:NCr-*Fox1*(*nu*) athymic mice. Animals (8 per group) were treated twice daily with vehicle or **51** once tumors reached a mean diameter of 5.3−5.4 mm. Tumour volumes and body weights were measured three times a week, and at the end of the study tumors were excised, weighed and snap frozen for PD analysis 6 and 24 h after the final dose.

Chemistry. Commercially available starting materials, reagents, and dry solvents were used as supplied. Flash column chromatography was performed using Merck silica gel 60 (0.025−0.04 mm). Column chromatography was also performed on a FlashMaster personal unit using isolute Flash silica columns or a Biotage SP1 purification system using Biotage Flash silica cartridges. Ion exchange chromatography was performed using acidic Isolute Flash SCX-II cartridges. ^{1}H NMR spectra were recorded on a Bruker Avance dpx250 or a Bruker Avance-500. Samples were prepared as solutions in a deuterated solvent and referenced to the appropriate internal nondeuterated solvent peak or tetramethylsilane. Chemical shifts were recorded in ppm (δ) downfield of tetramethylsilane. LC-MS spectra were recorded on a Waters LCT with a Waters Alliance 2795 separations module, using a Phenomenex Gemini C_{18} column and either of the following conditions: Method A (10 min) - nominal mass, LC injection with a 10 min gradient (MeOH and 0.1% formic acid), positive ionization and an injection volume of 3 μL. Column: Phenomenex Gemini C_{18} column (5 μm, 50 × 4.6 mm). Method B (6 min) - nominal mass, LC injection with a 6 min gradient (MeOH and 0.1% formic acid), positive ionization and an injection volume of 2 μL. Column: Phenomenex Gemini C_{18} column (3 μm, 30 × 4. Method C (3.5 min) - nominal mass, LC injection with a 3.5 min gradient (MeOH and 0.1% formic acid), positive ionization and an injection volume of 2 μL. Column: Phenomenex Gemini C_{18} column (3 μm, 30 × 4.6 mm). High resolution mass spectra were obtained using the above instrumental setup and the following conditions: Accurate mass, LC injection with a 10 min gradient (MeOH and 0.1% formic acid), +ve ionization and an injection volume of 4 μL. Column: Phenomenex Gemini C_{18} column (5 μm, 50 × 4.6 mm). Analytical HPLC analysis was performed on a Thermo-Finnigan Surveyor HPLC system at 30 °C, using a Phenomenex Gemini C_{18} column (5 μm, 50 × 4.6 mm) and 10 min gradient of 10 → 90% MeOH/0.1% formic acid, visualizing at 254, 309, or 350 nm. The purity of final compounds was determined by analytical HPLC as described above and is ≥95% unless specified otherwise. Elemental analyses were determined by Warwick Analytical Service Ltd., Coventry, UK.

5-Bromo-4-chloro-pyridin-2-ylamine (9). To a solution of 2-amino-4-chloropyridine (0.50 g, 3.9 mmol) in acetonitrile (20 mL) was added dropwise a solution of *N*-bromosuccinimide (0.730 g, 4.1 mmol) in acetonitrile (10 mL). The reaction mixture was stirred at room temperature for 16 h then concentrated in vacuo. The crude product was purified by chromatography on silica gel (hexane/ethyl acetate 6:4) to give the title compound as a white solid (0.65 g, 80%); ^{1}H NMR (250 MHz, $CDCl_3$) 4.50 (br s, 2H, NH_2), 6.63 (s, 1H) and 8.16 (s, 1H) (3-H, 6-H); LC (Method A) - MS (ESI, *m*/*z*) Rt = 4.8 min - 207, 209, 211 [(M + H^+), BrCl isotopic pattern].

5-Bromo-4-chloro-3-nitro-pyridin-2-ylamine (11). 5-Bromo-4-chloro-pyridin-2-ylamine (0.640 g, 3.0 mmol) was added in portions to conc. H_2SO_4 (6 mL) while the temperature was kept at below 10 °C. The reaction mixture was stirred at 5 to 10 °C for 15 min. The resulting solution was then heated at 55 °C, and HNO_3 (70%; 208 μL, 3.2 mmol) was dropwise added while the temperature was kept at 55−60 °C. The reaction mixture was stirred at 55 °C for 30 min then cooled to room temperature and poured slowly into ice (20 g). The pH was adjusted to 7 with 10% aqueous NaOH. The precipitated product was filtered, washed with water (20 mL), and dried in vacuo over P_2O_5 for 16 h to give the title compound as a yellow solid (0.580 g). Further purification of this product (0.48 g) by chromatography (hexane/ethyl acetate; v/v 7:3) gave the title compound as a yellow solid (0.287 g, 38%); ^{1}H NMR (250 MHz, $CDCl_3$) 5.78 (br s, 2H, NH_2), 8.29 (s, 1H, 6-H).

2-[4-(2-Amino-5-bromo-3-nitro-pyridin-4-yl)-piperazin-1-yl]-*N*-thiazol-2-yl-acetamide (13). To a mixture of 5-bromo-4-chloro-3-nitro-pyridin-2-ylamine (0.100 g, 0.39 mmol) and isopropanol (7 mL) was added 2-(piperazin-1-yl)-*N*-(thiazol-2-yl)acetamide × 2HCl salt (0.124 g, 0.41 mmol) and dry DIPEA (275 μL, 1.58 mmol). The mixture was heated at 50 °C for 16 h, then allowed to cool to room temperature, and concentrated in vacuo. The crude product was purified by chromatography on silica gel (hexane/ethyl acetate v/v 1:1, and a gradient of methanol (0 to 5%) in ethyl acetate) to give the title compound as a yellow solid (0.144 g, 82%); ^{1}H NMR (250 MHz, DMSO-d_6) 2.68 (broad t, J = 4.0 Hz, 4H, piperazine $N(CH_2)_2$), 3.10 (broad t, J = 4.0 Hz, 4H, piperazine $N(CH_2)_2$), 3.36 (s, 2H, NCH_2CO), 6.95 (broad s, 2H, NH_2), 7.22 (d, J = 3.6 Hz, 1H) and 7.47 (d, J = 3.6 Hz, 1H) (thiazole 4-H, 5-H), 8.16 (s, 1H, pyridine 6-H), 11.8 (broad s, 1H, CONH); LC (Method A) - MS (ESI, *m*/*z*) Rt = 4.69 min - 442, 444 [$(M + H)^+$, Br isotopic pattern].

2-{4-[6-Bromo-2-(4-dimethylaminophenyl)-3*H*-imidazo[4,5-*b*]-pyridin-7-yl]-piperazin-1-yl}-*N*-thiazol-2-yl-acetamide (15). To a mixture 2-[4-(2-amino-5-bromo-3-nitro-pyridin-4-yl)-piperazin-1-yl]-*N*-thiazol-2-yl-acetamide (0.100 g, 0.22 mmol) and ethanol (3 mL) was added 4-(dimethylamino)benzaldehyde (0.044 g, 0.29 mmol) and 1 M aq. $Na_2S_2O_4$ (900 μL, 0.9 mmol). The reaction mixture was stirred at reflux for 16 h then concentrated in vacuo. The crude product was purified by chromatography on silica gel (dichloromethane/ethyl acetate v/v 7:3, and then 0.5% to 2% methanol in ethyl acetate) to give the title compound as an off-white solid (0.034 g, 27%); ^{1}H NMR (250 MHz, DMSO-d_6) 2.77 (broad s, 4H, piperazine $N(CH_2)_2$), 2.99 (s, 6H, $N(CH_3)_2$), 3.40 (s, 2H, NCH_2CO), 3.67 (broad s, 4H, piperazine $N(CH_2)_2$), 6.82 (d, J = 8.8 Hz, 2H) and 8.02 (d, J = 8.8 Hz, 2H) 2,6-ArH and 3,5-ArH, 7.23 (d, J = 3.5 Hz, 1H) and 7.49 (d, 1H, J = 3.5 Hz) (thiazole 4-H, 5-H), 8.15 (s, 1H, imidazo[4,5-*b*]pyridine 5-H), 11.80 (broad s, 1H, CONH), 13.12 (broad s, 1H, imidazo[4,5-*b*]pyridine NH); LC (Method A)-MS (ESI, *m*/*z*) Rt = 6.0 min - 541, 543 [(M + H^+), Br isotopic pattern]; ESI-HRMS Found: 541.1132, calculated for $C_{23}H_{26}BrN_8OS$ $(M + H)^+$: 541.1128.

2-Amino-4,5-dichloro-3-nitropyridine (12). To a 50 mL round-bottomed flask containing 2-amino-4,5-dichloropyridine[30] (0.275 g, 1.65 mmol) and cooled into an ice-bath was slowly added conc. H_2SO_4 (2.79 g). The reaction mixture was stirred for 3 min and then HNO_3 (70%; 0.186 g) was dropwise added. The

reaction mixture was stirred at 0 °C (ice-bath) for 7 min, then heated to 55 °C and stirred at this temperature for 1 h, allowed to cool to room temperature, and diluted with ice−water (~15 mL), and the pH was adjusted to ~7.5 with 10% aqueous NaOH. The yellow precipitate was collected by filtration, washed with water, and dried in vacuo over P_2O_5, then absorbed on silica gel, and the free running powder was placed on a 10 g isolute silica column. Elution with 2% ethyl acetate in dichloromethane afforded the title compound as a yellow solid (0.090 g, 26%); ^{1}H NMR (250 Mz, DMSO-d_6) 7.39 (s, 2H, NH_2), 8.39 (s, 1H, 6-H).

2-(4-(2-Amino-5-chloro-3-nitropyridin-4-yl)piperazin-1-yl)-*N*-(thiazol-2-yl)acetamide (14). 2-(Piperazin-1-yl)-*N*-(thiazol-2-yl)-acetamide × 2HCl salt (0.209 g, 0.70 mmol) was suspended in ^{i}PrOH (12 mL) and DIPEA (0.295 g, 2.30 mmol). To this solution, 4,5-dichloro-3-nitropyridin-2-amine (0.130 g, 0.63 mmol) was added, and the reaction mixture was heated and stirred at 45 °C for 17 h. The mixture was then allowed to cool to room temperature, diluted with isopropanol (10 mL), filtered, washed with ^{i}PrOH (3 × 3 mL), Et_2O (2 × 5 mL), and dried to give the title compound as a yellow solid (0.200 g, 80%); ^{1}H NMR (500 MHz, DMSO-d_6): 2.68 (m, 4H, piperazine $N(CH_2)_2$), 3.10 (m, 4H, piperazine $N(CH_2)_2$), 3.38 (s, 2H, NCH_2CO), 6.95 (brs, 2H, NH_2), 7.22 (d, 1H, J = 2.5 Hz), 7.47 (d, 1H, J = 2.5 Hz) (thiazole 4-H and thiazole 5-H), 8.06 (s, 1H, pyridine 6-H), 11.98 (s, 1H, CONH); LC (Method B) - MS (ESI, *m*/*z*): Rt = 3.01 min −398, 400 [(M + H$^+$), Cl isotopic pattern]. The reaction was also performed using excess of 2-(piperazin-1-yl)-*N*-(thiazol-2-yl)-acetamide as a free base which was obtained from its hydrochloride salt as follows: 2-(Piperazin-1-yl)-*N*-(thiazol-2-yl)acetamide × 2HCl salt (0.360 g) was partitioned between saturated aqueous $NaHCO_3$ (40 mL) and ethyl acetate (30 mL). The aqueous layer was extracted with ethyl acetate (2 × 30 mL) and dichloromethane (5 × 25 mL). The combined organics were dried (Na_2SO_4) and then concentrated in vacuo to give 0.165 g of the free base.

2-(4-(6-Chloro-2-(4-(dimethylamino)phenyl)-3*H*-imidazo[4,5-*b*]-pyridin-7-yl)piperazin-1-yl)-*N*-(thiazol-2-yl)acetamide (7). To a mixture of 2-[4-(2-amino-5-chloro-3-nitro-pyridin-4-yl)-piperazin-1-yl]-*N*-thiazol-2-yl-acetamide (0.040 g, 0.10 mmol), ethanol (3 mL), and 4-(dimethylamino)benzaldehyde (0.019 g, 0.13 mmol) was added a freshly prepared aqueous solution of $Na_2S_2O_4$ (1M; 0.4 mL, 0.4 mmol). The reaction mixture was heated at 70 °C for 3.5 h, then allowed to cool to room temperature and the solvents were removed in vacuo. The residue was absorbed on silica gel, and the free running powder was placed on a 10 g isolute silica column which was eluted with ethyl acetate/dichloromethane (v/v; 1:1), 1.5% methanol in ethyl acetate/dichloromethane (v/v; 1:1), and finally 2% methanol in ethyl acetate/dichloromethane (v/v; 1:1). The title compound was obtained after trituration with diethyl ether as a pale yellow solid (0.005 g, 10%); ^{1}H NMR (250 MHz, DMSO-d_6) 2.78 (m, 4H, piperazine $N(CH_2)_2$), 3.01 (s, 6H, $N(CH_3)_2$), 3.40 (s, 2H, NCH_2CO), 3.72 (m, 4H, piperazine $N(CH_2)_2$), 6.83 (d, J = 8.8 Hz, 2H, 3,5-ArH or 2,6-ArH), 7.25 (d, J = 3.4 Hz, 1H) and 7.51 (d, J = 3.5 Hz, 1H) (thiazole 4-H, 5-H), 8.03 (d, 3H, J = 9.9 Hz, 3,5-ArH or 2,6-ArH, and imidazo[4,5-*b*]-pyridine 5-H); 11.95 (s, 1H, CONH), 13.12 (s, 1H, imidazo[4,5-*b*]-pyridine N−H); LC (Method A) − MS (ESI, *m*/*z*) 6.17 min −497, 499 [(M + H)$^+$, Cl isotopic pattern]; ESI-HRMS Found: 497.1652, calculated for $C_{23}H_{26}N_8ClOS$ (M + H)$^+$: 497.1633.

2-(4-(6-Cyano-2-(4-(dimethylamino)phenyl)-3*H*-imidazo[4,5-*b*]-pyridin-7-yl)piperazin-1-yl)-*N*-(thiazol-2-yl)acetamide (16). A solution of 2-(4-(6-bromo-2-(4-(dimethylamino)phenyl)-3*H*-imidazo-[4,5-*b*]pyridin-7-yl)piperazin-1-yl)-*N*-(thiazol-2-yl)acetamide (75 mg, 0.14 mmol) in degassed DMF (1 mL) containing Pd_2dba_3 (0.05 eq, 0.0069 mmol, 6 mg), dppf (0.1 eq, 0.014 mmol, 8 mg), and $Zn(CN)_2$ (1.5 eq, 0.21 mmol, 24 mg) was stirred with microwave heating at 180 °C for 30 min. After this time, further $Pd_2(dba)_3$ (6 mg), dppf (8 mg), and $Zn(CN)_2$ (24 mg) were added and the mixture was stirred under the same conditions for a further 30 min. HPLC then showed partial conversion to the desired compound. Concentration in vacuo and purification of a small sample by semipreparative HPLC gave the pure product as a colorless solid; ^{1}H NMR (500 MHz, DMSO-d_6) 2.80 (t, br, J = 4.7 Hz, 4H, piperazine $N(CH_2)_2$), 3.00 (s, 6H, $N(CH_3)_2$), 3.42 (s, 2H, NCH_2CO), 4.11 (s, br, 4H, piperazine $N(CH_2)_2$), 6.82 (d, J = 9.0 Hz, 2H, *N,N*-dimethylaminophenyl *H*-3 & *H*-5), 7.24 (d, J = 3.5 Hz, 1H, thiazole *H*-4 or *H*-5), 7.50 (d, J = 3.5 Hz, 1H, thiazole *H*-4 or *H*-5), 7.99 (d, J = 9.0 Hz, 2H, *N,N*-dimethylaminophenyl *H*-2 & *H*-6), 8.23 (s, 1H, imidazo[4,5-*b*]-pyridine *H*-5), 11.91 (br s, 1H, CON*H*), 13.46 (br s, 1H, imidazo-[4,5-*b*]pyridine N*H*); LC (Method A) - MS (ESI, *m*/*z*): 6.87 min - 488 [(M + H)$^+$, 100%]; ESI-HRMS: Found: 488.1993, calculated for $C_{24}H_{26}N_9OS$ (M+H)$^+$: 488.1981.

2-(4-(6-Chloro-2-(4-methoxyphenyl)-3*H*-imidazo[4,5-*b*]pyridin-7-yl)piperazin-1-yl)-*N*-(thiazol-2-yl)acetamide (27). To a mixture of 2-[4-(2-amino-5-chloro-3-nitro-pyridin-4-yl)-piperazin-1-yl]-*N*-thiazol-2-yl-acetamide (0.040 g, 0.10 mmol), ethanol (3 mL), and *p*-methoxybenzaldehyde (0.019 g, 0.14 mmol) was added a freshly prepared aqueous solution of $Na_2S_2O_4$ (1 M; 0.4 mL, 0.4 mmol). The reaction mixture was heated at 70 °C for 5 h, then allowed to cool to room temperature and the solvents were removed in vacuo. The residue was absorbed on silica gel and the free running powder was placed on a 10 g isolute silica column which was eluted with 50% dichloromethane in ethyl acetate and then 2.5% methanol in ethyl acetate/dichloromethane (v/v; 1:1). The title compound was obtained as a pale yellow solid after trituration with diethyl ether (0.012 g, 25%); ^{1}H NMR (500 MHz, DMSO-d_6) 2.76 (br s, 4H, piperazine $N(CH_2)_2$), 3.40 (s, 2H, NCH_2CO), 3.72 (br s, 4H, piperazine $N(CH_2)_2$), 3.83 (s, 3H, OCH_3), 7.10 (d, *J* = 8.8 Hz, 2H, 3,5-ArH or 2,6-ArH), 7.24 (d, *J* = 3.5 Hz, 1H) and 7.50 (d, *J* = 3.5 Hz, 1H) (thiazole 4-H, 5-H), 8.09 (s, 1H, imidazo[4,5-*b*]pyridine 5-H), 8.13 (d, *J* = 8.8 Hz, 2H, 3,5-ArH or 2,6-ArH), 11.95 (s, 1H, CONH), 13.38 (s, 1H, imidazo-[4,5-*b*]pyridine N−H) ; LC (Method A) - MS (ESI, *m*/*z*): Rt = 6.05 min −484, 486 [(M + H)$^+$, Cl isotopic pattern]. ESI-HRMS: Found: 484.1324, calculated for $C_{22}H_{23}ClN_7O_2S$ (M + H)$^+$: 484.1322.

2-(4-(2-Amino-5-chloro-3-nitropyridin-4-yl)piperazin-1-yl)-*N*-phenylacetamide (30b). To a mixture of 2-amino-4,5-dichloro-3-nitropyridine (0.031 g, 0.15 mmol) and isopropanol (3.5 mL) was added *N*-phenyl-2-piperazin-1-yl-acetamide × 2HCl salt (0.048 g, 0.16 mmol) followed by diisopropylethylamine (0.10 mL, 0.57 mmol). The reaction mixture was heated at 45 °C for 18 h, then allowed to cool to room temperature and the solvents were removed in vacuo. The residue was absorbed on silica gel and the free running powder was placed on a 10 g isolute silica column which was eluted with 10% to 30% ethyl acetate in dichloromethane. The title compound was obtained as a yellow solid (0.041 g, 71%); ^{1}H NMR (500 MHz, DMSO-d_6) 2.64 (br s, 4H, piperazine $N(CH_2)_2$), 3.13 (br s, 4H, piperazine $N(CH_2)_2$), 3.19 (s, 2H, NCH_2CO), 7.00 (br s, 2H, 2-NH_2), 7.06 (t, J = 7.3 Hz, 1H, *p*-Ar*H*), 7.31 (t, *J* = 8.3 Hz, 2H, *m*-Ar*H*), 7.63 (d, *J* = 7.3 Hz, 2H, *o*-Ar*H*), 8.07 (s, 1H, 6-H), 9.76 (s, 1H, CONH); LC (Method A) - MS (ESI, *m*/*z*): Rt = 4.50 min −391, 393 [(M + H)$^+$, Cl isotopic pattern].

2-(4-(6-Chloro-2-(4-(dimethylamino)phenyl)-3*H*-imidazo[4,5-*b*]-pyridin-7-yl)piperazin-1-yl)-*N*-phenylacetamide (31b). To a mixture of 2-(4-(2-amino-5-chloro-3-nitropyridin-4-yl)piperazin-1-yl)-*N*-phenylacetamide (0.040 g, 0.10 mmol), ethanol (3 mL), and 4-dimethylaminobenzaldehyde (0.019 g, 0.13 mmol) was added a freshly prepared aqueous solution of $Na_2S_2O_4$ (1 M; 0.40 mL, 0.40 mmol). The reaction mixture was heated at 70 °C for 3 h, then allowed to cool to room temperature and the solvents were removed in vacuo. The residue was absorbed on silica gel and the free running powder was placed on a 10 g isolute silica column which was eluted with 20% ethyl acetate in dichloromethane and then 1% methanol in ethyl acetate/dichloromethane (v/v; 1:1). The title compound was obtained as a yellow solid after trituration with diethyl ether (0.006 g, 12%); ^{1}H NMR (500 MHz, DMSO-d_6) 2.76 (br s, 4H, piperazine $N(CH_2)_2$), 3.00 (s, 6H, $N(CH_3)_2$), 3.23 (s, 2H, NCH_2CO), 3.75 (br s, 4H, piperazine $N(CH_2)_2$), 6.81 (d, J = 7.9 Hz, 2H), and 8.01 (d, J = 8.5 Hz, 2H)

(3,5-$C_6H_4NMe_2$ and 2,6-C_6H_4-NMe_2), 7.07 (t, J = 7.3 Hz, 1H, *p*-Ar*H*), 7.32 (t, J = 8.5 Hz, 2H, *m*-Ar*H*), 7.67 (d, J = 8.5 Hz, 2H, *o*-Ar*H*), 8.06 (s, 1H, imidazo[4,5-*b*]pyridine 5-H), 9.77 (s, 1H, CONH), 13.11 (s, 1H, imidazo[4,5-*b*]pyridine N−H); LC (Method B) - MS (ESI, *m*/*z*): Rt = 4.00 min −490, 492 [(M + H)$^+$, Cl isotopic pattern]. ESI-HRMS: Found: 490.2128, calculated for $C_{26}H_{29}ClN_7O$ (M + H)$^+$: 490.2122.

***tert*-Butyl 4-(2-amino-5-bromo-3-nitropyridin-4-yl)piperazine-1-carboxylate (17).** To a mixture of 5-bromo-4-chloro-3-nitropyridin-2-ylamine (0.126 g, 0.50 mmol) and isopropanol (9 mL) was added 1-BOC-piperazine (0.102 g, 0.55 mmol) followed by diisopropylethylamine (0.10 mL, 0.57 mmol). The reaction mixture was heated at 45 °C for 20 h, then allowed to cool to room temperature, and diluted with isopropanol (3 mL). The precipitate was collected by filtration and washed with isopropanol and diethyl ether. The title compound was thus obtained as a yellow solid (0.112 g, 56%). ^{1}H NMR (500 MHz, DMSO-d_6) 1.42 (s, 9H, $C(CH_3)_3$), 2.99 (br s, 4H, piperazine $N(CH_2)_2$), 3.45 (br s, 4H, piperazine $N(CH_2)_2$), 7.02 (s, 2H, NH_2), 8.20 (s, 1H, 6-H); LC (Method B) - MS (ESI, *m*/*z*): Rt = 5.00 min −402, 404 [(M + H)$^+$, Br isotopic pattern].

4-(2-Amino-5-bromo-3-nitropyridin-4-yl)-*N*-phenylpiperazine-1-carboxamide (30e). A solution of *tert*-butyl 4-(2-amino-5-bromo-3-nitropyridin-4-yl)piperazine-1-carboxylate (250 mg, 0.62 mmol) in CH_2Cl_2 (2.5 mL) at 0 °C was treated with TFA (2.5 mL) and stirred at 0 °C for 1.5 h. After this time, the solvents were evaporated in vacuo and the excess TFA was removed by azeotroping with toluene (3 × 10 mL). The residue was suspended in $CHCl_3$ (2.5 mL) and treated with DIPEA (5 eq, 3.11 mmol, 0.54 mL) and phenyl isocyanate (1.05 eq, 0.65 mmol, 0.07 mL). The reaction was warmed to room temperature and stirred for 12 h. The formed precipitate was filtered off and dried to give the product as a yellow solid (221 mg, 84% for two steps); ^{1}H NMR (500 MHz, DMSO-d_6) 3.07 (br s, 4H, piperazine $N(CH_2)_2$), 3.58 (br s, 4H, piperazine $N(CH_2)_2$), 6.94 (tt, J = 7.4, 1.1 Hz, 1H, phenyl *H*-4), 7.03 (br s, 2H, NH_2), 7.24 (dd, J = 8.5, 7.5 Hz, 2H, phenyl *H*-3 & *H*-5), 7.45 (dd, J = 8.5, 1.1 Hz, 2H, phenyl *H*-2 & *H*-6), 8.21 (s, 1H, pyridine *H*-6), 8.59 (br s, 1H, N*H*); LC (Method C) - MS (ESI, *m*/*z*): Rt = 2.34 min −421, 423 [(M + H)$^+$, Br isotopic pattern].

4-(6-Bromo-2-(4-(dimethylamino)phenyl)-3*H*-imidazo[4,5-*b*]-pyridin-7-yl)-*N*-phenylpiperazine-1-carboxamide (31e). A solution of 4-(2-amino-5-bromo-3-nitropyridin-4-yl)-*N*-phenylpiperazine-1-carboxamide (100 mg, 0.25 mmol) and 4-(dimethylamino)-benzaldehyde (1.05 eq, 0.26 mmol, 39 mg) in DMF (1.25 mL) was treated with a freshly prepared 1 M aqueous solution of $Na_2S_2O_4$ (3 eq, 0.75 mmol, 0.75 mL) and stirred at 80 °C for 4 h. After this time, the precipitate which had formed was filtered off and washed with hexane to give the product (64 mg, 53%) as an off-white solid; ^{1}H NMR (500 MHz, DMSO-d_6) 3.00 (s, 6H, $N(CH_3)_2$), 3.64−3.68 (m, 8H, 2 × piperazine $N(CH_2)_2$), 6.82 (d, *J* = 8.4 Hz, 2H, *N,N*-dimethylaminophenyl *H*-3 & *H*-5), 6.94 (t, *J* = 7.4 Hz, 1H, phenyl *H*-4), 7.25 (t, *J* = 7.5 Hz, 2H, phenyl *H*-3 & *H*-5), 7.51 (d, *J* = 8.2 Hz, 2H, phenyl *H*-2 & *H*-6), 8.02 (d, J = 8.2 Hz, 2H, *N,N*-dimethylaminophenyl *H*-2 & *H*-6), 8.20 (s, 1H, imidazo[4,5-*b*]-pyridine *H*-5), 8.61 (s, br, 1H, PhN*H*), 13.19 (s, br, 1H, imidazo[4,5-*b*]pyridine N*H*); LC (Method A) - MS (ESI, *m*/*z*): Rt = 8.34 min −520, 522 [(M + H)$^+$, bromine isotopic pattern). ESI-HRMS: Found: 520.1450, calculated for $C_{25}H_{27}BrN_7O$ (M + H)$^+$: 520.1460. Analytical hplc: (λ 254 nm) R_t 8.98 min, area 94.0%.

5-Chloro-3-nitro-4-(4-(pyridin-4-ylmethyl)piperazin-1-yl)pyridin-2-amine (intermediate for the synthesis of 36a). To a mixture of 2-amino-4,5-dichloro-3-nitropyridine (0.052 g, 0.25 mmol) and isopropanol (4.5 mL) was added 1-[(4-pyridyl)-methyl]-piperazine (0.049 g, 0.28 mmol) followed by diisopropylethylamine (0.05 mL, 0.28 mmol). The reaction mixture was heated at 45 °C for 24 h, then allowed to cool to room temperature, and diluted with isopropanol (3 mL). The formed precipitate was collected by filtration and washed with isopropanol and diethyl ether. The title compound was thus obtained as yellow solid (0.035 g). The filtrate was concentrated in vacuo, and purification of the residue on a isolute silica column using 0 to 5% methanol in ethyl acetate/dichloromethane (v/v; 1:1) as eluant gave an additional 0.036 g of the product (total yield: 81%); ^{1}H NMR (500 MHz, DMSO-d_6) 3.09 (br t, *J* = 4.4 Hz, 4H, piperazine $N(CH_2)_2$), 3.57 (s, 2H, NCH_2), 6.96 (s, 2H, NH_2), 7.34 (d, *J* = 5.8 Hz, 2H) and 8.51 (d, J = 5.9 Hz, 2H) (pyridine H-2 & H-6, H-3 & H-5), 8.06 (s, 1H, 6-H); LC (Method B) - MS (ESI, *m*/*z*): Rt = 1.95 min −349, 351 [(M + H)$^+$, Cl isotopic pattern].

6-Chloro-2-(4-methoxyphenyl)-7-(4-(pyridin-4-ylmethyl)piperazin-1-yl)-3*H*-imidazo[4,5-*b*]pyridine (36a). To a mixture of 5-chloro-3-nitro-4-(4-(pyridin-4-ylmethyl)piperazin-1-yl)pyridin-2-amine (0.031 g, 0.09 mmol) and ethanol (3.0 mL) was added 4-methoxybenzaldehyde (0.020 g, 0.14 mmol) with the aid of ethanol (1 mL) followed by a freshly prepared aqueous solution of $Na_2S_2O_4$ (1 M; 0.36 mL, 0.36 mmol). The reaction mixture was heated at 70 °C for 5 h, then allowed to cool to room temperature and the solvents were removed in vacuo. The residue was triturated with water, and the precipitate was collected by filtration, washed with water, ethanol, and diethyl ether. This material was further purified on a 10 g isolute silica column using a gradient of methanol (0 to 5%) in ethyl acetate/dichloromethane (v/v; 1:1) as eluant. The title compound was obtained as a pale yellow solid (0.007 g, 18%); ^{1}H NMR (500 MHz, DMSO-d_6) 2.61 (br s, 4H, piperazine $N(CH_2)_2$), 3.71 (br s, 4H, piperazine $N(CH_2)_2$), 3.61 (s, 2H, NCH_2), 3.83 (s, 3H, OCH_3), 7.09 (d, *J* = 8.8 Hz, 2H) and 8.12 (d, *J* = 8.8 Hz, 2H) (3,5-C_6H_4OMe and 2,6-C_6H_4−OMe), 7.40 (d, *J* = 5.8 Hz, 2H) and 8.54 (d, *J* = 4.5 Hz, 2H) (pyridine H-2 & H-6, H-3 & H-5), 8.08 (s, 1H, imidazo[4,5-*b*]pyridine 5-H), 13.37 (s, 1H, imidazo[4,5-*b*]-pyridine N−H); LC (Method B) - MS (ESI, *m*/*z*): Rt = 3.20 min −435, 437 [(M + H)$^+$, Cl isotopic pattern]. ESI-HRMS: Found: 435.1695, calculated for $C_{23}H_{24}ClN_6O$ (M + H)$^+$: 435.1700.

5-Bromo-3-nitro-4-(4-(pyridin-3-ylmethyl)piperazin-1-yl)pyridin-2-amine (38a). To a mixture of 5-bromo-4-chloro-3-nitropyridin-2-ylamine (0.126 g, 0.50 mmol) and isopropanol (9 mL) was added 1-[(3-pyridyl)-methyl]-piperazine (0.097 g, 0.55 mmol) followed by diisopropylethylamine (0.10 mL, 0.57 mmol). The reaction mixture was heated at 45 °C for 18 h, it was then allowed to cool to room temperature. The precipitate was collected by filtration and washed with isopropanol and diethyl ether. The title compound was thus obtained as a yellow solid (0.160 g, 82%); ^{1}H NMR (500 MHz, DMSO-d_6) 3.05 (br s, 4H, piperazine $N(CH_2)_2$), 3.56 (s, 2H, NCH_2), 7.02 (s, 2H, NH_2), 7.36 (dd, *J* = 7.8, 4.8 Hz, 1H, pyridyl 5-H), 7.74 (dt, *J* = 7.8, 1.70 Hz, 1H, pyridyl 4-H), 8.16 (s, 1H, 6-H), 8.47 (dd, *J* = 4.8, 1.6 Hz, 1H, pyridyl 6-H), 8.50 (d, *J* = 1.6 Hz, 1H, pyridyl 2-H); LC (Method B) - MS (ESI, *m*/*z*): Rt = 1.79 min −393, 395 [(M + H)$^+$, Br isotopic pattern].

6-Bromo-2-(4-morpholin-4-ylmethyl-phenyl)-7-(4-pyridin-3-ylmethyl-piperazin-1-yl)-3*H*-imidazo[4,5-*b*]pyridine (40a). To a mixture of 5-bromo-3-nitro-4-(4-pyridin-3-ylmethyl-piperazin-1-yl)-pyridin-2-ylamine (0.047 g, 0.12 mmol) and EtOH (3.5 mL) was added 4-(morpholin-4-ylmethyl)benzaldehyde (0.032 g, 0.16 mmol) followed by a freshly prepared aqueous solution of $Na_2S_2O_4$ (1 M; 0.48 mL, 0.48 mmol). The reaction mixture was stirred at 80 °C for 20 h, then allowed to cool to room temperature and concentrated in vacuo. The residue was absorbed on silica gel, the free-running powder was placed on a 10 g isolute silica column, and elution of the column with a gradient of methanol (2−12%) in ethyl acetate/dichloromethane (v:v; 4:1) afforded a yellow solid which was triturated with diethyl ether. The precipitate was collected by filtration and was successively washed with diethyl ether, water, and diethyl, then dried in vacuo (0.009 g, 14%). ^{1}H NMR (500 MHz, DMSO-d_6) 2.38 (br s, 4H), 2.62 (br s, 4H), 3.59 (t, *J* = 4.6 Hz, 4H) and 3.67 (br s, 4H) (morpholine $N(CH_2)_2$, morpholine $O(CH_2)_2$), and piperazine $N(CH_2)_2$), 3.53 (s, 2H) and 3.62 (s, 2H) (NCH_2-pyridyl and $C_6H_4CH_2$), 7.39 (dd, *J* = 5.3, 7.1 Hz, 1H, pyridine 5-H), 7.47 (d, J = 7.7 Hz, 2H) and 8.14 (d, *J* = 8.0 Hz, 2H) (3,5-C_6H_4 and 2,6-C_6H_4), 7.78 (d, J = 7.5 Hz, 1H, pyridine 4-H),

8.23 (s, 1H, imidazo[4,5-*b*]pyridine 5-H), 8.50 (dd, J = 1.6, 4.7 Hz, 1H, pyridine 6- H), 8.56 (d, J = 1.6 Hz, 1H, pyridine 2-H), 13.48 (br s, 1H, imidazo[4,5-*b*]pyridine N−H); LC (Method B) - MS (ESI, m/z): Rt = 1.94 min −548, 550 [$(M + H)^+$, Br isotopic pattern]. ESI-HRMS: Found: 548.1776, calculated for $C_{27}H_{31}BrN_7O$ $(M + H)^+$: 548.1773.

5-Bromo-4-(4-(4-chlorobenzyl)piperazin-1-yl)-3-nitropyridin-2-amine (38c). To a mixture of 5-bromo-4-chloro-3-nitro-pyridin-2-ylamine (0.126 g, 0.50 mmol) and isopropanol (15 mL) was added 1-(4-chlorobenzyl)piperazine (0.115 g, 0.55 mmol) followed by diisopropylethylamine (0.10 mL, 0.55 mmol). The reaction mixture was heated at 45 °C for 18 h, then allowed to cool to room temperature. The precipitate was collected by filtration and washed with isopropanol and diethyl ether. The title compound was thus obtained as a yellow solid (0.148 g, 70%); ^{1}H NMR (500 MHz, DMSO-d_6) 3.05 (br s, 4H, piperazine $N(CH_2)_2$), 3.52 (s, 2H, NCH_2), 7.02 (s, 2H, NH_2), 7.34 (d, J = 8.5 Hz, 2H) and 7.38 (d, J = 8.5 Hz, 2H) (3,5-ArH and 2,6-ArH), 8.16 (s, 1H, 6-H); LC (Method B) - MS (ESI, m/z): Rt = 2.92 min −426, 428, 430 [$(M + H)^+$, BrCl isotopic pattern].

6-Bromo-7-[4-(4-chlorobenzyl)-piperazin-1-yl]-2-(4-morpholin-4-ylmethyl-phenyl)-3*H*-imidazo[4,5-*b*]pyridine (40c). To a mixture of 5-bromo-4-[4-(4-chlorobenzyl)-piperazin-1-yl]-3-nitro-pyridin-2-ylamine (0.060 g, 0.14 mmol) and EtOH (6.5 mL) was added 4-(morpholin-4-ylmethyl)benzaldehyde (0.040 g, 0.19 mmol) followed by a freshly prepared aqueous solution of $Na_2S_2O_4$ (1 M; 0.63 mL, 0.63 mmol). The reaction mixture was stirred at 80 °C for 20 h, then allowed to cool to room temperature and concentrated in vacuo. The residue was absorbed on silica gel, the free-running powder was placed on a 10 g isolute silica column and elution with a gradient of methanol (0−8%) in ethyl acetate/dichloromethane (v:v; 1:1) afforded a yellow solid. The title compound was obtained as a pale yellow solid after trituration with diethyl ether (0.038 g, 46%). ^{1}H NMR (500 MHz, DMSO-d_6) 2.38 (br s, 4H), 2.61 (br s, 4H) 3.59 (t, J = 4.5 Hz, 4H), and 3.66 (br s, 4H) (piperazine $N(CH_2)_2$, morpholine $N(CH_2)_2$ and morpholine $O(CH_2)_2$), 3.54 (s, 2H) and 3.57 (s, 2H) (NCH_2-C_6H_4Cl and $C_6H_4CH_2$), 7.41 (m, 4H, C_6H_4Cl), 7.47 (d, J = 8.2 Hz, 2H) and 8.14 (d, J = 8.2 Hz, 2H) (3,5-C_6H_4 and 2,6-C_6H_4), 8.23 (s, 1H, imidazo[4,5-*b*]pyridine 5-H), 13.48 (br s, 1H, imidazo[4,5-*b*]pyridine N−H); LC (Method B) - MS (ESI, m/z): Rt = 2.55 min −581, 583, 585 [$(M + H)^+$, BrCl isotopic pattern]. ESI-HRMS: Found: 581.1424, calculated for $C_{28}H_{31}BrClN_6O$ $(M + H)^+$: 581.1426. This compound was also converted to its hydrochloride salt as follows: To a mixture of **40c** (0.021 g, 0.036 mmol) and dichloromethane (1.0 mL) was slowly added a solution of HCl in methanol (1.25 M; 1.1 mL). The resulting clear solution was stirred at room temperature for 2 min, then diethyl ether (15 mL) was added. The white precipitate was collected by filtration, washed with diethyl ether and dried in vacuo over P_2O_5 to afford the title compound (0.020 g) as a 3 × HCl salt. LC (Method B) - MS (ESI, m/z): Rt = 2.55 min −581, 583, 585 [$(M + H)^+$, BrCl isotopic pattern]; Anal. ($C_{28}H_{30}BrClN_6O$ × 3HCl × $2H_2O$) Cl; calcd 19.50, found 19.38.

4-(5-Methyl-isoxazol-3-ylmethyl)-piperazine-1-carboxylic acid *tert*-butyl ester (43e). To a solution of 3-bromomethyl-5-methyl-isoxazole (0.102 g, 0.58 mmol) in dichloromethane (6 mL) was added 1-BOC-piperazine (0.240 g, 1.30 mmol). The reaction mixture was stirred at room temperature for 18 h under argon, then concentrated in vacuo. The resulting residue was absorbed on silica and the free-running powder was placed on a 10 g isolute silica column. Elution with a gradient of ethyl acetate (30 to 70%) in petroleum ether (60−80 °C) afforded the title compound as a white solid (0.124 g, 76%). ^{1}H NMR (500 MHz, DMSO-d_6) 1.39 (s, 9H, $C(CH_3)_3$), 2.32 (t, J = 5.1 Hz, 4H, piperazine $N(CH_2)_2$), 2.38 (s, 3H, isoxazole 5-CH_3), 3.35 (br t, 4H, piperazine $N(CH_2)_2$), 3.50 (s, 2H, NCH_2 isoxazole), 6.17 (s, 1H, isoxazole 4-H); LC (Method B) - MS (ESI, m/z): Rt = 2.60 min −282 [$(M + H)^+$, 5%], 226 [$(M - {}^tBu)^+$, 100%].

5-Bromo-4-[4-(5-methyl-isoxazol-3-ylmethyl)-piperazin-1-yl]-3-nitro-pyridin-2-ylamine (38e). A solution of 4-(5-methyl-isoxazol-3-ylmethyl)-piperazine-1-carboxylic acid *tert*-butyl ester (0.200 g, 0.71 mmol) in dichloromethane (6 mL) and TFA (8 mL) was stirred at room temperature for 2 h then concentrated in vacuo, and the resulting residue was dried in vacuo to give **37e**. This material (supposedly 0.70 mmol) was dissolved in isopropanol (13 mL) and to this solution 2-amino-5-bromo-4-chloro-3-nitropyridine (0.157 g, 0.63 mmol) was added followed by diisopropylethylamine (0.65 mL, 3.70 mmol). The reaction mixture was stirred at 45 °C for 20 h, then allowed to cool to room temperature and diluted with isopropanol (5 mL). The resulting orange solid was collected by filtration, washed with isopropanol (2 × 5 mL), diethyl ether (3 × 5 mL), and dried (0.170 g, 68%); ^{1}H NMR (500 MHz, DMSO-d_6) 2.38 (s, 3H, isoxazole 5-CH_3), 2.53 (br s, 4H, piperazine $N(CH_2)_2$), 3.05 (br s, 4H, piperazine $N(CH_2)_2$), 3.55 (s, 2H, NCH_2-isoxazole), 6.21 (s, 1H, isoxazole 4-H), 6.97 (s, 2H, NH_2), 8.16 (s, 1H, pyridine 6-H); LC (Method B) - MS (ESI, m/z): Rt = 2.67 min −397, 399 [$(M + H)^+$, Br isotopic pattern].

6-Bromo-2-(4-methoxyphenyl)-7-[4-(5-methyl-isoxazol-3-ylmethyl)-piperazin-1-yl]-3*H*-imidazo[4,5-*b*]pyridine (39e). To a mixture of 5-bromo-4-[4-(5-methyl-isoxazol-3-ylmethyl)-piperazin-1-yl]-3-nitro-pyridin-2-ylamine (0.044 g, 0.11 mmol) and EtOH (3 mL) was added 4-methoxybenzaldehyde (0.023 g, 0.17 mmol) with the aid of EtOH (1 mL), followed by a freshly prepared aqueous solution of $Na_2S_2O_4$ (1 M; 0.44 mL, 0.44 mmol). The reaction mixture was stirred at 70 °C for 18 h, then allowed to cool to room temperature and concentrated in vacuo. The resulting residue was absorbed on silica, and the free-running powder was placed on a 10 g isolute silica column. Elution with ethyl acetate/dichloromethane (v:v; 3:7) and then 2.5% methanol in ethyl acetate/dichloromethane (v:v; 1:1) afforded a yellow solid. The title compound was obtained as a pale yellow solid after trituration with diethyl ether (0.023 g, 43%); ^{1}H NMR (500 MHz, DMSO-d_6) 2.40 (s, 3H, isoxazole 5-CH_3), 2.64 (br s, 4H, piperazine $N(CH_2)_2$), 3.60 (s, 2H, NCH_2), 3.65 (br s, 4H, piperazine $N(CH_2)_2$), 3.84 (s, 3H, OCH_3), 6.25 (s, 1H, isoxazole 4-H), 7.10 (d, J = 8.9 Hz, 2H) and 8.13 (d, J = 8.8 Hz, 2H) (3,5-C_6H_4OMe and 2,6-C_6H_4OMe), 8.20 (s, 1H, imidazo[4,5-*b*]-pyridine 5-H), 13.35 (br s, 1H, imidazo[4,5-*b*]pyridine N−H); LC (Method B) - MS (ESI, m/z): Rt = 3.80 min −483, 485 [$(M + H)^+$, Br isotopic pattern]. ESI-HRMS: Found: 483.1150, calculated for $C_{22}H_{24}BrN_6O_2$ $(M + H)^+$: 483.1144.

3-((4-(6-Bromo-2-(4-(4-methylpiperazin-1-yl)phenyl)-3*H*-imidazo-[4,5-*b*]pyridin-7-yl)piperazin-1-yl)methyl)-5-methylisoxazole (51). To a mixture of 5-bromo-4-(4-((5-methylisoxazol-3-yl)methyl)piperazin-1-yl)-3-nitropyridin-2-amine (0.052 g, 0.13 mmol) and EtOH (5 mL) was added 4-(4-methylpiperazino)benzaldehyde (0.032 g, 0.16 mmol) followed by a freshly prepared aqueous solution of $Na_2S_2O_4$ (1 M; 0.52 mL, 0.52 mmol). The reaction mixture was stirred at 80 °C for 18 h, then allowed to cool to room temperature and concentrated in vacuo. The residue was absorbed on silica gel, and the free-running powder was placed on a 10 g isolute silica column. Elution with ethyl acetate/chloroform (v:v; 1:1), and then a gradient of methanol (5−12%) in chloroform afforded a yellow solid. This solid was triturated with diethyl ether, and the formed yellow precipitate was collected by filtration and was successively washed with diethyl ether, water, and diethyl ether. The title compound was obtained as a pale yellow solid (0.022 g, 31%). ^{1}H NMR (500 MHz, DMSO-d_6) 2.23 (s, 3H, piperazine N-Me), 2.40 (s, 3H, isoxazole 5-CH_3), 2.46 (br t, J = 4.8 Hz, 4H), 2.63 (br s, 4H), 3.27 (br s obscured by water peak), and 3.63 (br t, J = 4.7 Hz, 4H) (piperazine NCH_2), 3.60 (s, 2H, N−CH_2-isoxazole), 6.25 (s, 1H, isoxazole 4-H), 7.06 (d, J = 9.0 Hz, 2H), and 8.02 (d, J = 8.9 Hz, 2H) (2,6-C_6H_4 and 3,5-C_6H_4), 8.17 (s, 1H, imidazo[4,5-*b*]-pyridine 5-H), 13.20 (br s, 1H, imidazo[4,5-*b*]pyridine N−H); LC (Method B) - MS (ESI, m/z): Rt = 2.33 min −551, 553 [$(M + H)^+$, Br isotopic pattern]. ESI-HRMS: Found: 551.1870, calculated for $C_{26}H_{32}BrN_8O$ $(M + H)^+$: 551.1877.

Acknowledgment. The authors are grateful to Chroma Therapeutics, and in particular to Dr. D. Moffat, for valuable discussions, the kinase selectivity profiling of **40c**, and the provision of bulk intermediates **11** and **17**. We acknowledge NHS funding to the NIHR Biomedical Research Centre. This work was supported by Cancer Research UK [CUK] grant number C309/A8274. R.B. is a Royal Society University Research Fellow and acknowledges the support of Breakthrough Breast Cancer Project Grant AURA 05/06 and infrastructural support for Structural Biology at the ICR from Cancer Research UK. We also thank Dr. Amin Mirza and Mr. Meirion Richards for their assistance with NMR, mass spectrometry, and HPLC.

Supporting Information Available: Experimental procedures for compounds **18−26**, **28**, **29d**, **29i**, **30c**, **30d**, **30f−l**, **31a**, **31c**, **31d**, **31f−l**, **33**, **35**, **36b**, **37b**,**g**, **42b**,**g**, **37f**,**h**, **43f**,**h**, **38b**,**d**, **38f−h**, **39a−d**, **39f−h**, **40b**, **40e**, **40g**, **40h**, **44−50**, **52−54**, summary of crystallographic analysis of compounds **40c** and **51** (Table S1) and kinase selectivity profiling of compound **51** (Table S2). This material is available free of charge via the Internet at http://pubs.acs.org.

References

(1) Carmena, M; Earnshaw, W. C. The Cellular Geography of Aurora Kinases. *Nat. Rev. Mol. Cell Biol.* **2003**, *4*, 842–854.
(2) Ducat, D.; Zheng, Y. Aurora Kinases in Spindle Assembly and Chromosome Segregation. *Exp. Cell Res.* **2004**, *301*, 60–67.
(3) Marumoto, T.; Zhang, D.; Saya, H. Aurora-A, A Guardian of Poles. *Nat. Rev. Cancer* **2005**, *5*, 42–50.
(4) Bishop, J. D.; Schumacher, J. M. Phosphorylation of the Carboxyl Terminus of Inner Centromere Protein (INCENP) by Aurora B Kinase Stimulates Aurora B Kinase Activity. *J. Biol. Chem.* **2002**, *277*, 27577–27580.
(5) Giet, R.; Glover, D. M. Drosophila Aurora B Kinase Is Required for Histone H3 Phosphorylation and Condensin Recruitment During Chromosome Condensation and to Organise the Central Spindle During Cytokinesis. *J. Cell Biol.* **2001**, *152*, 669–682.
(6) Keen, N.; Taylor, S. Aurora-Kinase Inhibitors as Anticancer Agents. *Nat. Rev. Cancer* **2004**, *4*, 927–936.
(7) Matthews, N.; Visintin, C.; Hartzoulakis, B.; Jarvis, A.; Selwood, D. L. Aurora A and B Kinases As Targets for Cancer: Will They be Selective For Tumors? *Exp. Rev. Anticancer Ther.* **2006**, *6*, 109–120.
(8) Gautschi, O.; Heighway, J.; Mack, P. C.; Purnell, P. R.; Lara, P. N., Jr.; Gandara, D. R. Aurora Kinases as Anticancer Drug Targets. *Clin. Cancer Res.* **2008**, *14*, 1639–1648.
(9) Tanaka, T.; Kimura, M.; Matsunaga, K.; Fukada, D.; Mori, H.; Okano, Y. Centrosomal Kinase AIK1 is Overexpressed in Invasive Ductal Carcinoma of the Breast. *Cancer Res.* **1999**, *59*, 2041–2044.
(10) Bischoff, J. R.; Anderson, L.; Zhu, Y.; Mossie, K.; Ng, L.; Souza, B.; Schryver, B.; Flanagan, P.; Clairvoyant, F.; Ginther, C.; Chan, C. S. M.; Novotny, M.; Slamon, D. J.; Plowman, G. D. A Homologue of Drosophila Aurora Kinase Is Oncogenic and Amplified in Human Colorectal Cancers. *EMBO J.* **1998**, *17*, 3052–3065.
(11) Gritsko, T. M.; Coppola, D.; Paciga, J. E.; Yang, L.; Sun, M.; Shelley, S. A.; Fiorica, J. V.; Nicosia, S. V.; Cheng, J. Q. Activation and Overexpression of Centrosome Kinase BTAK/Aurora-A in Human Ovarian Cancer. *Clin. Cancer. Res.* **2003**, *9*, 1420–1426.
(12) Reichardt, W.; Jung, V.; Brunner, C.; Klein, A.; Wemmert, S.; Romeike, B. F. M.; Zang, K. D.; Urbschat, S. The Putative Serine/Threonine Kinase Gene STK15 on Chromosome 20q13.2 Is Amplified in Human Gliomas. *Oncol. Rep.* **2003**, *10*, 1275–1279.
(13) Zhou, H.; Kuang, J.; Zhong, L.; Kuo, W.; Gray, J. W.; Sahin, A.; Brinkley, B. R.; Sen, S. Tumour Amplified Kinase ST15/BTAK Induces Centrosome Amplification, Aneuploidy, and Transformation. *Nat. Genet.* **1998**, *20*, 189–193.
(14) Chieffi, P.; Troncone, G.; Caleo, A.; Libertini, S.; Linardopoulos, S.; Tramontano, D.; Portella, G. Aurora B Expression in Normal Testis and Seminonas. *J. Endocrinol.* **2004**, *181*, 263–270.
(15) Araki, K.; Nozaki, K.; Ueba, T.; Tatsuka, M.; Hashimoto, N. High Expression of Aurora-B/Aurora and Ipl1I-like Midbody-Associated Protein (AIM-1) in Astrocytomas. *J. Neurooncol.* **2004**, *67*, 53–64.
(16) Sorrentino, R.; Libertini, S.; Pallante, P. L.; Troncone, G.; Palombini, L.; Bavetsias, V.; Cernia, D. S.; Laccetti, P.; Linardopoulos, S.; Chieffi, P.; Fusco, A.; Portella, G. Aurora B Overexpression Associates with the Thyroid Carcinoma Undifferentiated Phenotype and Is Required for Thyroid Carcinoma Cell Proliferation. *J. Clin. Endocrinol. Metab.* **2005**, *90*, 928–935.
(17) Ota, T.; Suto, S.; Katayama, H.; Han, Z-B; Suzuki, F.; Maeda, M.; Tanino, M.; Terada, Y.; Tatsuka, M. Increased Mitotic Phosphorylation of Histone H3 Attributable to AIM-1/Aurora-B Overexpression Contributes to Chromosome Number Instability. *Cancer Res.* **2002**, *62*, 5168–5177.
(18) Takahashi, T.; Futamura, M.; Yoshimi, N.; Sano, J.; Katada, M.; Takagi, Y.; Kimura, M.; Yoshioka, T.; Okano, Y.; Saji, S. Centrosomal Kinases, HsAIRK1 and HsAIRK3, Are Overexpressed in Primary Colorectal Cancers. *Jpn. J. Cancer Res.* **2000**, *91*, 1007–1014.
(19) Pollard, J. R.; Mortimore, M. Discovery and Development of Aurora Kinase Inhibitors As Anticancer Agents. *J. Med. Chem.* **2009**, *52*, 2629–2651.
(20) Harrington, E. A.; Bebbington, D.; Moore, J.; Rasmussen, R. K.; Ajose-Adeogun, A. O.; Nakayama, T.; Graham, J. A.; Demur, C.; Hercend, T.; Diu-Hercend, A.; Su, M.; Golec, J. M. C.; Miller, K. M. VX-680, a Potent and Selective Small-Molecule Inhibitor of the Aurora Kinases, Suppresses Tumor Growth in Vivo. *Nat. Med.* **2004**, *10*, 262–267.
(21) Fancelli, D.; Moll, J.; Varasi, M.; Bravo, R.; Artico, R.; Berta, D.; Bindi, S.; Cameron, A.; Candiani, I.; Cappella, P.; Carpinelli, P.; Croci, W.; Forte, B.; Giorgini, M. L.; Klapwijk, J.; Marsiglio, A.; Pesenti, E.; Roccheti, M.; Roletto, F.; Severino, D.; Soncini, C.; Storici, P.; Tonani, R.; Zugnoni, P.; Vianello, P. 1,4,5,6-Tetrahydropyrrolo[3,4-*c*]pyrazoles: Identification of a Potent Aurora Kinase Inhibitor With a Favorable Antitumor Kinase Inhibition Profile. *J. Med. Chem.* **2006**, *49*, 7247–7251.
(22) Caprinelli., P.; Ceruti, R.; Giorgini, M. L.; Cappella, P.; Gianellini, L.; Croci, V.; Degrassi, A.; Texido, G.; Rocchetti, M.; Vianello, P.; Rusconi, L.; Storici, P.; Zugnoni, P.; Arrigoni, C.; Soncini, C.; Alli, C.; Patton, V.; Marsiglio, A.; Ballinari, D.; Pesenti, E.; Fancelli, D.; Moll, J. PHA-739358, a Potent Inhibitor of Aurora Kinases With a Selective Target Inhibition Profile Relevant to Cancer. *Mol. Cancer Ther.* **2007**, *6*, 3158–3168.
(23) Howard, S.; Berdini, V.; Boulstridge, J. A.; Carr, M. G.; Cross, D. M.; Curry, J.; Devine, L. A.; Early, T. R.; Fazal, L.; Gill, A. L.; Heathcote, M.; Maman, S.; Matthews, J. E.; McMenamin, R. L.; Navarro, E. F.; O'Brien, M. A.; O'Reilly., M.; Rees, D. C.; Reule, M.; Tisi, D.; Williams, G.; Vinković, M; Wyatt, P. G. Fragment-Based Discovery of the Pyrazol-4-yl urea (AT9283), a Multitargeted Kinase Inhibitor With Potent Aurora Kinase Activity. *J. Med. Chem.* **2009**, *52*, 379–388.
(24) Oslob, J. D.; Romanowski, M. J.; Allen, D. A.; Baskaran, S.; Bui, M.; Elling, R. A.; Flanagan, W. M.; Fung, A. D.; Hanan, E. J.; Harris, S.; Heumann, S. A.; Hoch, U.; Jacobs, J. W.; Lam, J.; Lawrence, C. E.; McDowell, R. S.; Nannini, M. A.; Shen, W.; Silverman, J. A.; Sopko, M. M.; Tangonan, B. T.; Teague, J.; Yoburn, J. C.; Yu, C. H.; Zhong, M.; Zimmerman, K. M.; O'Brien, T.; Lew, W. Discovery of a Potent and Selective Aurora Kinase Inhibitor. *Bioorg. Med. Chem. Lett.* **2008**, *18*, 4880–4884.
(25) Manfredi, M. G.; Ecsedy, J. A.; Meetze, K. A.; Balani, S. K.; Burenkova, O.; Chen, W.; Galvin, K. M.; Hoar, K. M.; Huck, J. J.; LeRoy, P. J.; Ray, E. T.; Sells, T. B.; Stringer, B.; Stroud, S. G.; Vos, T. J.; Weatherhead, G. S.; Wysong, D. R.; Zhang, M.; Bolen, J. B.; Claiborne, C. F. Antitumour Activity of MLN8054, an Orally Active Small-Molecule Inhibitor of Aurora A Kinase. *Proc. Natl. Acad. Sci. U.S.A.* **2007**, *104*, 4106–4111.
(26) Mortlock, A. A.; Foote, K. M.; Heron, N. M.; Jung, F. H.; Pasquet, G.; Lohmann, J-J. M.; Warin, N.; Renaud, F.; De Savi, C.; Roberts, N. J.; Johnson, T.; Dousson, C. B.; Hill, G. B.; Perkins, D.; Hatter, G.; Wilkinson, R. W.; Wedge, S. R.; Heaton, S. P.; Odedra, R.; Keen, N. J.; Crafter, C.; Brown, E.; Thompson, K.; Brightwell, S.; Khatri, L.; Brady, M. C.; Kearney, S.; McKillop, D.; Rhead, S.; Parry, T.; Green, S. Discovery, Synthesis, and *in Vivo* Activity of a New Class of Pyrazoloquinazolines as Selective Inhibitors of Aurora B Kinase. *J. Med. Chem.* **2007**, *50*, 2213–2224.
(27) Bavetsias, V.; Sun, C.; Bouloc, N.; Reynisson, J.; Workman, P.; Linardopoulos, S.; McDonald, E. Hit generation and exploration: Imidazo[4,5-*b*]pyridine Derivatives as Inhibitors of Aurora Kinases. *Bioorg. Med. Chem. Lett.* **2007**, *17*, 6567–6571.
(28) Chan, F.; Sun, C.; Perumal, M.; Nguyen, Q.-D.; Bavetsias, V.; McDonald, E.; Martins, V.; Wilsher, N.; Valenti, M.; Eccles, S.; te Poele, R.; Workman, P.; Aboagye, E. O.; Linardopoulos, S. Mechanism of Action And *in Vivo* Quantification of Biological Activity of the Aurora Kinase Inhibitor CCT129202. *Mol. Cancer Ther.* **2007**, *6*, 3147–3157.
(29) Yang, D.; Fokas, D.; Li, J.; Yu, L.; Baldino, C. M. A Versatile Method for the Synthesis of Benzimidazoles from *o*-Nitroanilines

and Aldehydes in One Step via a Reductive Cyclization. *Synthesis* **2005**, 47–56.
(30) Gudmundsson, K. S.; Hinkley, J. M.; Brieger, M. S.; Drach, J. C.; Townsend, L. B. An Improved Large Scale Synthesis of 2-Amino-4-chloropyridine and Its Use for The Convenient Preparation of Various Polychlorinated 2-Aminopyridines. *Synth. Commun.* **1997**, *27*, 861–870.
(31) Wallace, D. J.; Chen, C. Cyclopropylboronic Acid: Synthesis and Suzuki Cross-Coupling Reactions. *Tetrahedron Lett.* **2002**, *43*, 6987–6990.
(32) Bellezza, F.; Cipiciani, A.; Cruciani, G.; Fringuelli, F. The Importance of Ester and Alkoxy Type Functionalities for the Chemo- and Enantio-Recognition of Substrates by Hydrolysis With *Candida Rugosa* Lipase. *J. Chem. Soc. Perkin 1* **2000**, 4439–4444.
(33) Tret'yakova, A. V.; Rudaya, L. I.; El'tsov, A. V. Acid-base Properties of Isomeric 2-Arylimidazopyridines. *Zhurnal Obshchei Khimii* **1984**, *54*, 2617–2620.
(34) Dalvie, D. K.; Kalgutkar, A. S.; Khojasteh-Bakht, S. C.; Obach, R. S.; O'Donnell, J. P. Biotransformation Reactions of Five-Membered Aromatic Heterocyclic Rings. *Chem. Res. Toxicol.* **2002**, *15*, 269–298.
(35) Blagg, J. Structure-Activity Relationships for *In Vitro* and *In Vivo* Toxicity. *Annu. Rep. Med. Chem.* **2006**, *41*, 353–369.
(36) Kalgutkar, A. S.; Dalvie, D. K.; O'Donnell, J. P.; Taylor, T. J.; Sahakian, D. C. On the Diversity of Oxidative Bioactivation Reactions on Nitrogen-Containing Xenobiotics. *Curr. Drug Metab.* **2002**, *3*, 379–424.
(37) Nutley, B. P.; Smith, N. F.; Hayes, A.; Kelland, L. R.; Brunton, L.; Golding, B. T.; Smith, G. C.; Martin, N. M.; Workman, P.; Raynaud, F. I. Preclinical Pharmacokinetics and Metabolism of a Novel Prototype DNA-PK Inhibitor NU7026. *Br. J. Cancer* **2005**, *93*, 1011–1018.
(38) CLogP was calculated using ChemBioDraw 11.00 Ultra by CambridgeSoft (www.cambridgesoft.com).
(39) Bayliss, R.; Sardon, T.; Vernos, I.; Conti, E. Structural Basis of Aurora-A Activation by TPX2 at the Mitotic Spindle. *Mol. Cell* **2003**, *12*, 851–862.
(40) CCP4. The CCP4 (Collaborative Computational Project Number 4) Suite: Programmes for Protein Crystallography. *Acta Crystallogr. D Biol. Crystallogr.* **1994**, *50*, 760-763.
(41) Adams, P. D.; Grosse-Kunstleve, R. W.; Hung, L. W.; Ioerger, T. R.; McCoy, A. J.; Moriarty, N. W.; Read, R. J.; Sacchettini, J. C.; Sauter, N. K.; Terwilliger, T. C. PHENIX: Building New Software for Automated Crystallographic Structure Determination. *Acta Crystallogr. D Biol. Crystallogr.* **2002**, *58*, 1948–1954.
(42) Moreno-Farre, J.; Workman, P.; Raynaud, F. I. Analysis of Potential Drug-Drug Interactions for Anticancer Agents in Human Liver Microsomes by High Throughput Liquid Chromatography/Mass Spectrometry Assay. *Austral.-Asian J. Cancer* **2007**, *6*, 55–68.